



**NTNU – Trondheim**  
Norwegian University of  
Science and Technology

# Open Conductor Faults and Dynamic Analysis of a Power System

**Simon Jorums Mabeta**

Master of Science in Electric Power Engineering

Submission date: June 2012

Supervisor: Kjetil Uhlen, ELKRAFT

Co-supervisor: Professor Trond Toftevag, ELKRAFT

Norwegian University of Science and Technology  
Department of Electric Power Engineering





**NTNU – Trondheim**  
Norwegian University of  
Science and Technology

# OPEN CONDUCTOR FAULTS AND DYNAMIC ANALYSIS OF AN ELECTRIC POWER SYSTEM

Simon Jorums Mabeta

Master of Science in Electric Power Engineering

Supervisor: Kjetil Uhlen

Co Supervisor: Trond Toftevaag

Thesis Submission Date: 11<sup>th</sup> June 2012

Department of Electric Power Engineering

(This page was intentionally left blank)

## Abstract

The overall goal of this thesis is to study and understand Open Conductor Faults and to assess their impact on the stability of a power system. In particular, the thesis has investigated the effect of this type of the fault on the dynamic electromechanical behavior of synchronous machine. The thesis has also focused on the effect of generator and transformer grounding as well as the effect of transformer winding configuration on the stability of the power system during this type of fault.

Open conductor faults are series faults which involve a break in one or two of the three conductors of a three phase power system. As such, the fault is an unsymmetrical fault and thus, the theory of symmetrical components was revisited. Symmetrical components and symmetrical circuits have been used to analyze both types of open conductor faults in order to understand the phenomenon and ease calculations.

A dual approach to this study has been undertaken. The phenomenon is treated analytically through calculations and then the calculated results are confirmed through computer simulations using SIMPOW, a power system simulation software. In either approach, it is evidently clear, through the use of Eigen values and calculated damping coefficients, that the damping of the machine in an open conductor situation is worse than the for the normal case without the fault.

A research in to the developed equations for damping has been undertaken. The theory of induction motors is applied in development of both the positive and negative damping power. The equation for negative damping power is developed first, using the symmetrical component concept and secondly, using the single phasing concept.

In the investigation of transformer winding configurations and the grounding generators and transformers, different scenarios have been considered and simulated in order to show their effect during the fault.

Finally the two open conductor case has also been investigated analytically and through computer simulation. The effect of grounding is shown in the results obtained. It shows that power transfer only occurs when there is a return path from the point of the fault to the generator.

(This page was intentionally left blank)

## Acknowledgements

I wish to thank my supervisor Professor Kjetil Uhlen for according me the opportunity to undertake a research on this interesting topic. I also wish to thank him for the technical assistance and guidance he rendered to me. Finally, I wish to acknowledge the motivation and support I got from him. He truly made me feel at home.

Secondly, I thank my co-supervisor Professor Trond Toftevaag for the technical assistance and the follow up communication on the thesis work as well as the assistance with SIMPOW simulation software. I thank him for all the books and the papers that he gave me access to in order to do this work. He always managed to find time to attend to me on those many occasions despite his busy schedule.

Thirdly, I wish to thank my mother Catherine and my brother Raymond for the moral support that they gave me during this study. They gave me a reason to soldier on. Indeed, blood is thicker than water.

Finally, I wish to dedicate this thesis to Tapewa, my nephew. It is my hope that this work will help to motivate him to achieve all that he may want to achieve in his life. This is for you.

(This page was intentionally left blank)



# Contents

1. Introduction.....	2
1.1 Motivation .....	2
1.2 Objectives .....	3
1.3 Scope of Work .....	3
1.4 Choice of Power System Model.....	3
1.5 Choice of the synchronous machine .....	4
1.6 SIMPOW .....	4
1.7 Outline of the Thesis .....	4
2. Theory.....	6
2.1 Open Conductor Faults.....	6
2.1.1 One Open Conductor fault .....	6
2.1.2 Two Open Conductors.....	7
2.1.3 General Observations.....	9
2.2 Power System Grounding and Transformer Winding Configurations.....	9
2.2.1 Synchronous Machines.....	9
2.2.2 Transformers .....	9
2.2.3 Transmission Lines.....	10
2.3 Synchronous Machine and the Power-Angle Characteristic Curve.....	11
2.3.1 Synchronous Machine Parameters.....	11
2.3.2 The Swing Equation .....	12
2.3.3 The Power Angle Characteristic of a system .....	13
2.4 Damping and the Induction Machine Theory.....	14
2.4.1 Synchronous Machine .....	14
2.4.2 The Polyphase Induction Motor .....	14
2.4.3 Single Phase Induction Motor .....	15
2.5 Power System Stability.....	17
2.5.1 Steady State Stability Analysis.....	17
2.5.2 Transient Stability Analysis.....	18
3. Damping .....	21
3.1 Power System Network Description.....	21
3.2 Positive Damping.....	22
3.2.1 Positive Damping Equation .....	22
3.2.2 Application to the Open Conductor Case.....	24
3.2.3 Application to the Two Open Conductor Case.....	24
3.3 Negative Damping .....	25
3.3.1 Negative Damping Equation: Symmetrical Components Concept.....	25
3.3.2 Negative Damping Equation: Single Phasing Concept .....	27
3.4 Discussion .....	28
4. Power Angle Characteristic Curve of the Synchronous Generator – Case Study.....	29
4.1 Analytically .....	29
4.2 Using SIMPOW.....	30
4.3 Discussion .....	31
5. Damping Coefficient - Case Studies.....	32
5.1 Description of the case studies .....	32
5.2 Calculation of Damping Coefficient - Analytically .....	33
5.3 Using a Type 4 Synchronous Generator model in SIMPOW.....	35
5.4 Using a Type 2A Synchronous Generator model in SIMPOW .....	35

5.5 Discussion .....	36
6. Transient Stability: Case studies.....	37
6.1 Analytically .....	37
6.2 SIMPOW simulation results.....	42
6.3 Discussion .....	44
7. Effect of Power System Grounding and Transformer Winding Configuration: Case Studies.....	45
7.1 Power System Grounding.....	45
7.2 Transformer Winding Configuration .....	49
7.2.1 Analytically .....	49
7.2.2 SIMPOW Simulation .....	50
7.3 Discussion .....	51
8. Two Open Conductors Fault: Case Studies.....	52
8.1 Analytically .....	53
8.1.1 Effect of grounding.....	54
8.1.2 Effect of Transformer winding configuration.....	54
8.2 Simulation using SIMPOW .....	55
8.2.1 Effect of grounding.....	56
8.2.2 Effect of transformer winding configuration.....	57
8.3 Discussion .....	58
9. Discussion.....	59
10. Conclusions.....	60
11. Recommendations and Further work .....	61
12. References.....	62
13. Appendices .....	64
13.1 Appendix A: Synchronous Machine Parameters.....	65
13.2 Appendix B: SIMPOW Files for Power Angle Characteristic curve .....	66
13.3 Appendix C: Power-Angle Curves for Round Rotor Synchronous Machine .....	69
13.4 Appendix D: SIMPOW files for damping coefficient simulation.....	70
13.5 Appendix E: SIMPOW files for Transient stability simulation .....	74
13.6 Appendix F: DYNPOW file for power system grounding simulation .....	77
13.7 Appendix G: DYNPOW file winding configuration simulation.....	79
13.8 Appendix H: DYNPOW file for two open-conductor fault simulation .....	81
13.9 Appendix I: Power Angle Characteristic curves using SIMPOW for case study in chapter 4	83

## Symbols, Abbreviations and Keywords

OCF – Open Conductor Fault

SMIB – Single Machine Infinite Bus

SIMPOW – Power system simulation software

Optpow – Power flow file in SIMPOW

Dynpow – Dynamic file in SIMOW

mmf – magnetic field

(This page was intentionally left blank)

# 1. Introduction

This report outlines the work which was undertaken in the final semester of my 2 year Master's Program. The thesis work was a continuation of the project work which was done in the previous semester in the TET5500 course [1].

## 1.1 Motivation

The occurrence of two incidents of this type of fault in 2008 initiated the proposal to study this fault in more detail in the 2009 project and the 2010 thesis work by Sjøholt [2]. The two faults occurred on an actual Nord Trøndelag Electricity network and this affected generators at the NKF power station. The initial proposal was to investigate the fault of 7<sup>th</sup> March 2008 which led to the uncontrolled oscillations and subsequent disconnection of all three generators at NFK power station. This was simulated using a simple model in SIMPOW and the work was extended to cover the larger NTE power system network in the Thesis. The scope also included generator protection schemes available in case of the occurrence of this fault.

The work was thus conducted for a particular case and though different scenarios were cover to assess the problem in totality, it was confined to a particular network with specific machine and network parameters and configuration. It was recommended that further work be carried out on smaller network models with different parameters for lines, transformers and generators. . It is for this reason that it was decided in this project work to conduct an initial investigation of the effect of this type of a fault on a single machine connected directly to an infinite grid. After an intense study on this simple network, a systematic development was made on the network to include a line, then later a transformer between the generator and the infinite grid. The study was also extended to induction machines.

During the study of the previous thesis work, it was observed that not much literature existed on the subject of open conductor faults and the effect on the power system. It was recommended that further work is undertaken to research more on the sources.

## 1.2 Objectives

The main objective of this thesis was to study and understand Open Conductor Faults and assess their impact on the stability of a power system. In particular, the thesis investigated the effect of this type of the fault on the dynamic electromechanical behavior of synchronous machine. It also focused on the effect of generator and transformer grounding as well as the effect of transformer winding configuration on the stability of the power system during this type of fault.

## 1.3 Scope of Work

The scope of work for the project can be summarized as follows:

- a) Further research on the theory of Open Conductor Faults and symmetrical components.
- b) Further study and use of the SIMPOW simulation software.
- c) Analytic analysis of the damping of a synchronous machine under the fault condition.
- d) Analysis of the Power Angle characteristic curve during Open Conductor Fault condition
- e) Investigation of the effect of grounding of the synchronous generator and transformer on the dynamic behavior of the synchronous generator during the fault.
- f) Research on the effect of this type of fault on an induction machine.

## 1.4 Choice of Power System Model

Various configurations of a power system were set up depending on the area of interest. The degree of complexity also varied depending on the matter to be investigated.

The most basic and simple single machine connected directly to the grid was analyzed first in order to understand the behavior of the machine and develop the equations for damping, open conductor voltage and phase currents. A transmission line, at the generated voltage, was then added to the system. This was done in order to understand the impact of the line reactance on the damping of the system. Finally, a generator transformer was added to the network. This was used to simulate the grounding and transformer winding effect on the open conductor fault. The transmission line also had a zero sequence reactance which was also useful in assessing the earthing aspect.

## 1.5 Choice of the synchronous machine

In the Specialization Project [1], the synchronous machine which was used was the same as the one used in the Power System Stability course [20]. From the massive inertia constant and the other machine parameters outlined in chapter 3 of the Specialization Project, it was noticed that the machine was a thermal unit. In order to relate to figures and parameters in the simulation, it was decided to change the machine to a hydroelectric power unit.

## 1.6 SIMPOW

The simulation tool which was chosen for use is SIMPOW mainly due to its availability at NTNU. It is a highly integrated software package developed by Swedish STRI for simulation of power systems [3]. It is currently owned by Manitoba HVDC Research Center.

The basic functions of Simpow include Load-flow calculation, Short-circuit calculation, Synchronous stability, Transient and Voltage stability, Prime mover torque irregularities, Machine dynamics, Sub synchronous resonance, Resonance frequency analysis by means of Eigenvalues and Eigenvectors, Frequency and Parameter scanning, Modal analysis and Harmonics Analysis.

## 1.7 Outline of the Thesis

This thesis is arranged as follows:

- Chapter 1 introduces the thesis with an account of how an actual incident resulted in to a proposal to undertake a research on this kind of fault. As such, an account of the previous work is given. It also outlines the objectives of this thesis and the scope of work.
- Chapter 2 gives a brief account of the theory related to the thesis topic.
- Chapter 3 is an account of the research that was undertaken to come up with the damping of a synchronous machine during an open conductor. It also gives an account of the simulation which was done using SIMPOW to verify the derived damping constant.
- Chapter 4 is about the Power-Angle Characteristic curves of a synchronous machine in the normal case as well as during an open conductor fault.
- Chapter 5 gives an account of the different scenarios that serve to demonstrate the effect of other parameters on the stability of the system due to this kind of fault.
- Chapter 6 is a discussion of the transient stability case which was investigated.

- Chapter 7 is about the effect of external impedance and grounding on the stability of a power system during an open conductor situation.
- Chapter 8 covers the two open conductor case study.
- Chapter 9 discusses the findings and chapter 10 gives a conclusive remark.
- Chapter 11 gives an account of recommendations for further work on this topic

Finally there are appendices for the extra material which has been referred to in the report.



## 2. Theory

### 2.1 Open Conductor Faults

Open conductor conditions in a balanced three phase circuit may be caused by a blown fuse or by a deliberate single pole switching operation. Similar conditions occur when there is a physical break in one or two of the three transmission line conductors due to an accident such as a tree fall or a storm. This condition results in an unbalance and thus, asymmetrical currents flow in the circuit.

Since the fault is an unsymmetrical fault, the analysis is best done with the use of symmetrical components and sequence networks. A detailed matrix approach has been demonstrated in section 12.6 of Grainger and Stevenson [4]. This matrix approach is a good tool for analysis of a network with so many nodes. For smaller networks like the ones used in this thesis, the approach that has been used in this thesis is the one used in section 13.4.6 of Machowski [5], section 3.7 of Reddy [6], section 2.8 of Das [7], chapter VI of Kimbark [8] and section 13.4.6 of Kundur [18].

#### 2.1.1 One Open Conductor fault

This fault involves a break in one of the three conductors as has been exemplified by the figure below. This shows a section of a three phase system between nodes  $m$  and  $n$ , with phase  $a$  open between points  $p$  and  $p'$ .

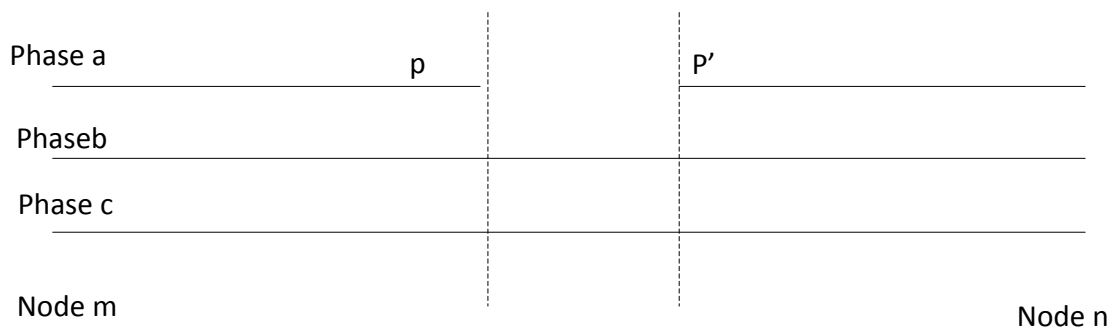


**Figure 1: Schematic diagram showing a Section of a three phase transmission line with an open conductor in line  $a$  between point  $p$  and  $p'$**

The representation of this type of fault using symmetrical components is as follows, assuming an open conductor occurs in conductor  $a$ :

$$I_a = 0 \quad (1)$$

$$V_b = V_c = 0 \quad (2)$$

Where  $I_a$  is the current flowing in conductor  $a$  after the fault and  $V_b$  and  $V_c$  are the series voltage drops between the points  $p$  and  $p'$ . Resolving these equations in to symmetrical components gives:

$$I_a^{(0)} + I_a^{(1)} + I_a^{(2)} = 0 \quad (3)$$

$$V_a^{(0)} = V_a^{(1)} = V_a^{(2)} = \frac{V_{pp',a}}{3} \quad (4)$$

Equation 3 demonstrates that an open conductor in one phase of a three phase network causes equal voltage drops to appear from point  $p$  to  $p'$  in the sequence networks. Equation 4 demonstrates that the voltage drops of the separate sequence are equal. These two equations suggest that the sequence networks are connected in parallel as shown below.

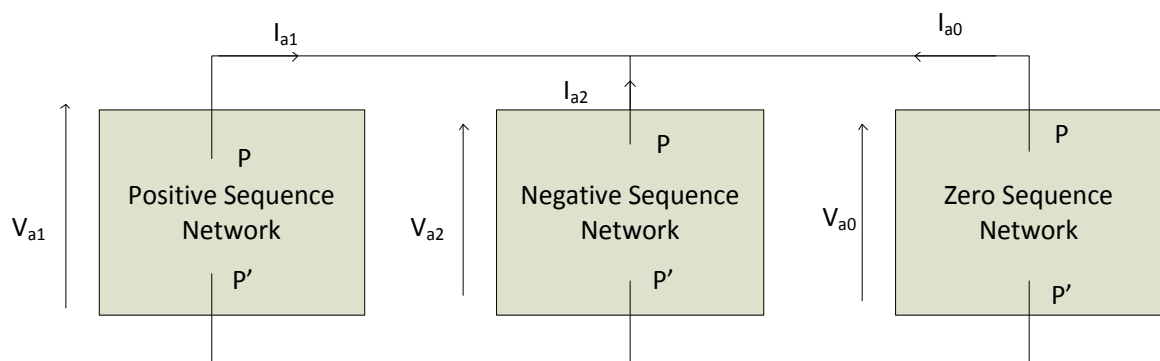
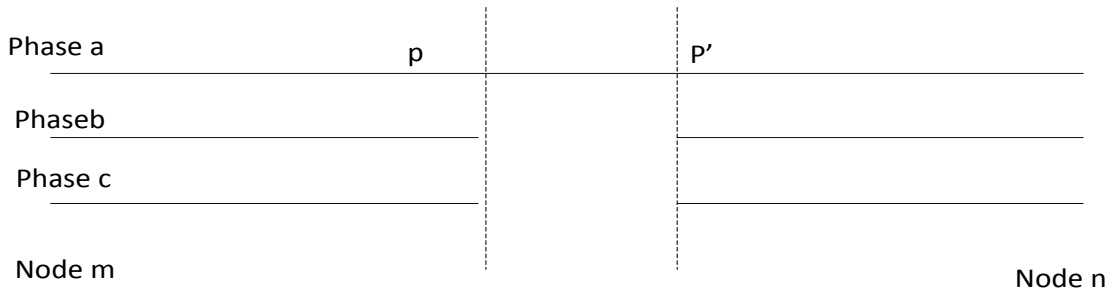


Figure 2: Connection of sequence networks to simulate one open conductor fault between  $p$  and  $p'$

### 2.1.2 Two Open Conductors

This fault involves a break in two of the three conductors. A schematic diagram is shown below.



**Figure 3: Schematic showing a Section of a three phase transmission line with an open conductor in phases *b* and *c* between point *p* and *p'***

For two open conductors between points *p* and *p'*, the conditions are satisfied by the following equations, assuming an open conductor occurs in conductors *b* and *c*:

$$V_a = 0 \tag{5}$$

$$I_b = I_c = 0 \tag{6}$$

The representation of this fault using symmetrical components is as follows:

$$V_a^{(0)} + V_a^{(1)} + V_a^{(2)} = 0 \tag{7}$$

$$I_a^{(0)} + I_a^{(1)} + I_a^{(2)} = \frac{I_a}{3} \tag{8}$$

The sequence network connection which satisfies the above equations is a series connection of the sequence networks as shown in the figure below.

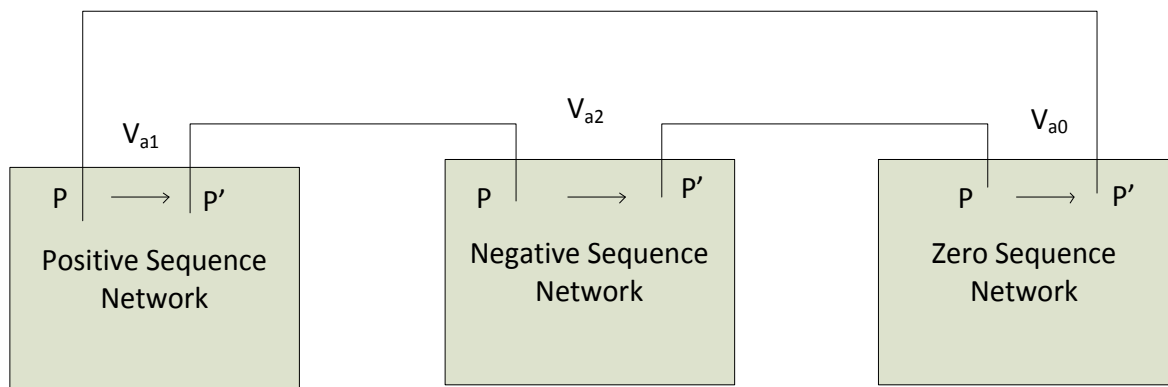


**Figure 4: Connection of the sequence networks of a system to simulate open conductors *b* and *c* between *p* and *p'***

### 2.1.3 General Observations

The parallel connection of the sequence networks in the One Open Conductor case shown in figure 2 demonstrates that there is power transfer through the line between points  $p$  and  $p'$  even if the zero sequence network has an infinite impedance. However, in the Two Open Conductor case, the transfer of power only occurs when the zero sequence circuit provides a path with finite impedance.

## 2.2 Power System Grounding and Transformer Winding Configurations

Methods of grounding a power system affect the zero sequence impedance networks. As such, grounding has an effect on the unsymmetrical fault currents in the network. Components which are grounded on the network include the rotating machines, transformers and transmission lines.

### 2.2.1 Synchronous Machines

A synchronous machine may be grounded through an impedance, or it may be solidly ground or it may be ungrounded. The positive sequence circuit is represented by a voltage behind a reactance circuit.

### 2.2.2 Transformers

Most three phase power systems consist either of three identical single-phase transformers connected in Y or delta or of a three phase transformer with the windings connected in Y or delta. The transformer may be grounded or ungrounded. Grounding of the transformer is done through the neutral of the Y connected winding either solidly or through an impedance [8].

The transformer can be represented in sequence networks by a positive, negative and zero sequence networks. The positive network consists of a series impedance and an ideal transformer of complex ratio. The negative sequence network is identical to the positive except that the angle of the ideal transformer is opposite sign. The zero sequence circuit depends on the winding of the transformer as well as grounding. These are summarized in section 11.8 of Grainger and Stevenson [4] and section 13.4.5 of Kundur [18] and quoted below.

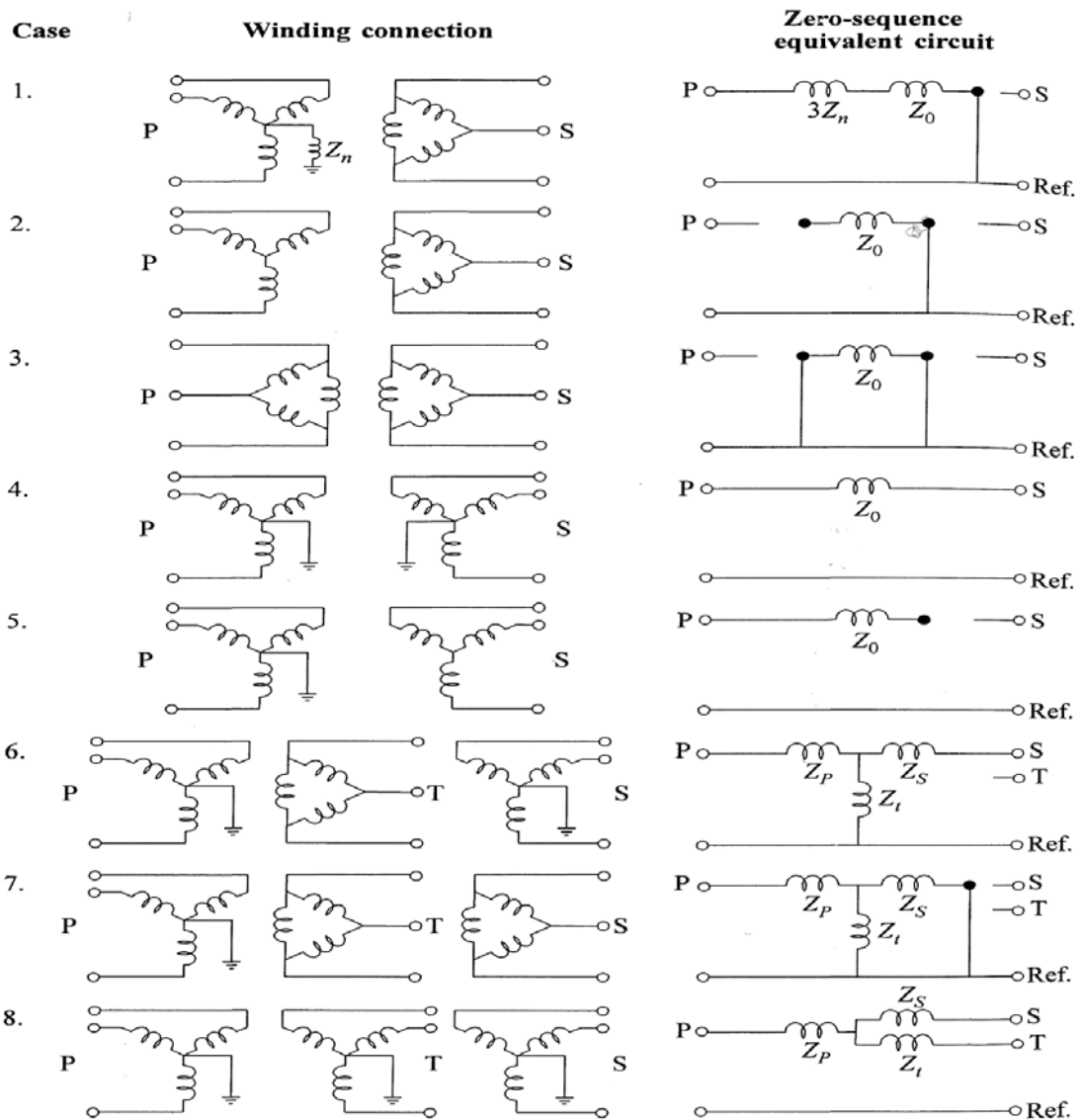


Figure 5: Zero sequence circuit for different transformer winding configurations

### 2.2.3 Transmission Lines

The positive, negative and zero sequence circuits are represented by impedances in the line model. The positive and negative impedances are dependent on the line conductors and normally identical. The zero sequence impedance is dependent on the grounding and earthing conductors of the line. Thus the impedance for the zero sequence is usually higher than the other two sequence networks.

## 2.3 Synchronous Machine and the Power-Angle Characteristic Curve

### 2.3.1 Synchronous Machine Parameters

The theory on machine parameters is detailed in chapter XII of Kimbark [9]. These include the following reactances, time constants and resistances.

- Direct-axis reactance  $x_d$
- Quadrature-axis reactance  $x_q$
- Armature leakage reactance  $x_l$ . This has been neglected in most applications
- Direct-axis transient reactance  $x_d'$
- Direct-axis subtransient reactance  $x_d''$
- Quadrature-axis transient reactance  $x_q'$
- Quadrature-axis subtransient reactance  $x_q''$
- Negative Sequence reactance. This is related to the movement of the mmf wave at twice the synchronous speed and thus is related to  $x_d''$  and  $x_q''$ . It is estimated as the arithmetic mean of  $x_d''$  and  $x_q''$  in Kimbark [9] and the square root of the the product of the same two parameters in Machowski et al [5]. The arithmetic estimates are shown in the equations below.

$$x_2 = \frac{x_d'' + x_q''}{2} \quad (9)$$

And,

$$x_2 = \sqrt{x_d'' x_q''} \quad (10)$$

respectively.

- Zero sequence reactance  $x_0$ .
- Positive sequence resistance  $r_1$ . This is usually neglected except in the calculation of the negative sequence damping in this thesis.
- Negative sequence resistance  $r_2$ . This is greater than the positive sequence resistance. The value depends on the value of the amortisseur windings when present as discussed in chapter XIV of Kimbark [9].
- Zero sequence resistance  $r_0$ . This depends on rotor copper loss due to currents induced by zero sequence currents. For a grounded Y connected winding, the resistance includes three times the resistance of the grounding resistor.
- Direct-axis transient open-circuit and short circuit constants,  $T_{d0}'$  and  $T_d'$
- Direct-axis subtransient open-circuit and short circuit constants,  $T_{d0}''$  and  $T_d''$
- Quadrature-axis time constants  $T_{q0}'$ ,  $T_q'$ ,  $T_{q0}''$  and  $T_q''$ .

### 2.3.2 The Swing Equation

The synchronous machine is a rotating body and thus the laws of mechanics apply to it [8]. The swing equation is a dynamic representation of the synchronous machine and it has parameters such as mass, electrical connection of the machine to the rest of the network, damping information as well as the mechanical input or output ([5] and [18]). It shows that the product of angular acceleration and moment of inertia equals the accelerating torque as expressed below:

$$I\alpha = T_{in} - T_{out} \quad (11)$$

Where  $\alpha$  is the angular acceleration

$T_{in}$  is the shaft torque

$T_{out}$  is the electromagnetic torque

$I$  is the moment of inertia of the machine

Equation 11 neglects losses and the effect of damping. Multiplying the expression by the speed  $\omega$  and then, expressing the angular acceleration  $\alpha$  as the rate of change of angle  $\delta$ , gives:

$$M \frac{d^2 \delta}{dt^2} = P_a = P_{in} - P_{out} \quad (12)$$

Where:  $M$  is the angular momentum

$P_{in}$  is the shaft power input

$P_{out}$  is the electrical power

$P_a$  is the acceleration power

Mechanical and electrical losses have been neglected.

As explained in Machowski et al [5], it is common practice to express the angular momentum in terms of the normalized Inertia constant  $H$ . When the damping is included, the equation expressed in per unit, takes the common form as follows:

$$2H \frac{d^2 \delta}{dt^2} = P_a = P_{in} - P_{out} - P_D \quad (13)$$

or as:

$$2H \frac{d^2 \delta}{dt^2} = P_m - P_e - P_D \quad (14)$$

### 2.3.3 The Power Angle Characteristic of a system

The maximum power a synchronous machine can deliver is determined by the maximum torque which can be applied without loss of synchronism with the external system to which it is connected [16]. For the single machine connected to an infinite grid as shown below:

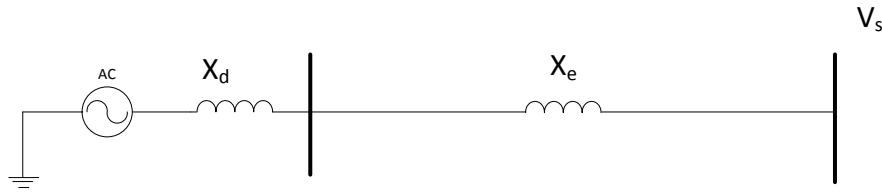


Figure 6: Equivalent circuit of synchronous machine connected to an infinite grid through a line.

The power delivery to the system is expressed as follows:

$$P_e = \frac{E_q V_s}{x_d} \sin \delta + \frac{V_s^2}{2} \frac{x_d - x_q}{x_d x_q} \sin 2\delta \quad (15)$$

Where  $x_d = X_d + X_e$

$x_q = X_q + X_e$

For the transient power angle characteristic, the equation becomes:

$$P_e = \frac{E_q V_s}{x'_d} \sin \delta + \frac{V_s^2}{2} \frac{x'_d - x'_q}{x'_d x'_q} \sin 2\delta \quad (16)$$

Where  $x'_d = X'_d + X_e$

$X'_q = X'_q + X_e$

It is important to understand how the dynamic characteristic of a generator is located with respect to the static characteristic on the power-angle diagram. For a given stable equilibrium point, where  $P_e = P_m$ , the balance of power must be held whichever characteristic is considered so that both the static and dynamic characteristic must intersect at the equilibrium point [5]



## 2.4 Damping and the Induction Machine Theory

### 2.4.1 Synchronous Machine

The two principal types of damper windings are as described in chapter XIV of Kimbark [9]. These are complete (or connected) and Incomplete (or non-connected). The end conductors of the complete windings for all the poles are connected through an end ring at either end while for the latter type, the damper windings of each pole are in an independent grid.

The other classification for the windings is according to their resistance. They could either be Low-resistance or High-resistance damper windings. Low resistance produce the highest torque at low slip while the later produces high torque at large slips. The reasons for damper windings are listed in [9] and shown here as follows:

1. To provide starting torque
2. To suppress hunting
3. To damp oscillations
4. To prevent distortion of the voltage wave shape and balance the terminal voltages
5. To prevent overheating of the pole pieces
6. To provide a braking torque on a generator during unsymmetrical faults
7. To provide additional torque for synchronizing generators
8. To reduce circuit breaker recovery voltage rates
9. To reduce the stress on the insulation of the field winding

Of much interest to this thesis, are the reasons listed as number 2, 3 and 6. The effect of this damping action can be best explained by the Induction-motor theory

### 2.4.2 The Polyphase Induction Motor

The induction motor can be thought of as a transformer whose magnetic circuit is separated by an air gap in to two relatively movable portions [20]. The stator is connected to alternating currents supply and this induces a rotating magnetic flux in the air gap. The flux links with the secondary winding on the rotor which is short circuited, or closed through an external resistance. The essential feature which distinguishes the induction motor from other electric motors is that the secondary currents are created solely by induction just like in the transformer secondary winding.

The ratio of the rotor speed to the synchronous speed of the stator flux is called the slip,  $s$ . This slip is used to express the secondary parameters of resistance and reactance when referred to the primary side. The equivalent circuit is as shown below.

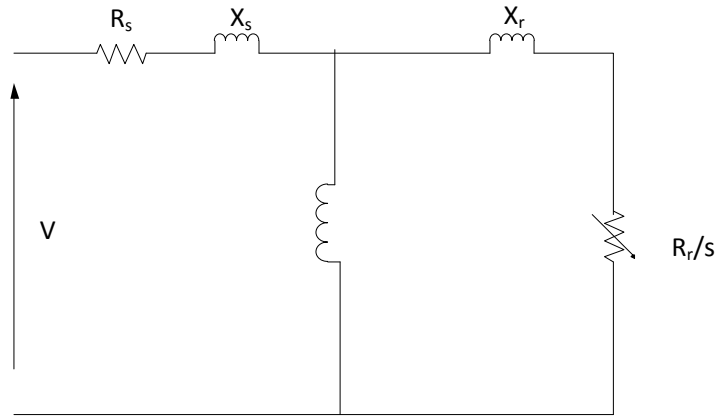


**Figure 7: Induction Motor equivalent circuit.**

Where  $V$  is the voltage applied to the stator

$R_s$  is the stator resistance

$X_s$  is the stator reactance

$X_r$  is the rotor reactance

$R_r$  is the rotor resistance

$s$  is the slip.

### 2.4.3 Single Phase Induction Motor

The stator mmf wave of a single phase induction motor is shown to be equivalent to two constant amplitude mmf waves revolving in opposite directions at synchronous speed [16]. Each of these component waves induces its own component rotor currents and produces induction-motor action just like a balanced polyphase motor.

The circuit diagram below is a representation of the double revolving field concept, where one half revolves in the forward and the other in the backward direction, both with half the amplitude.

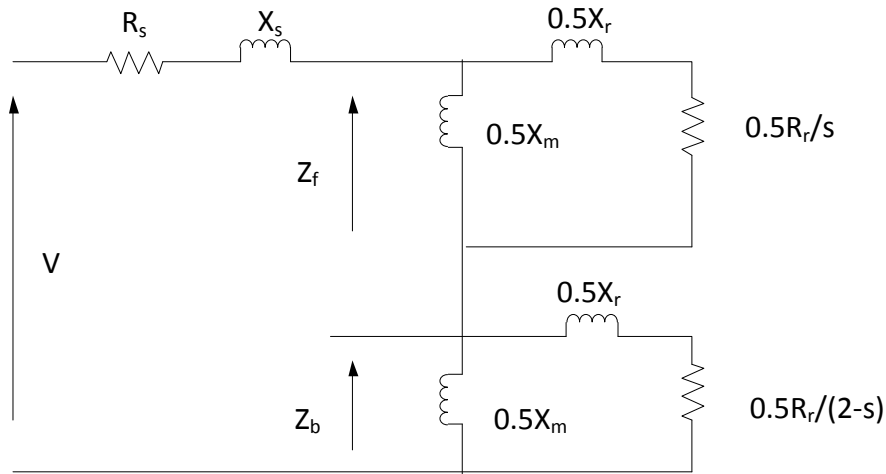


**Figure 8: Equivalent circuit of a single phase induction Motor.**

Where  $V$  is the voltage connected to the single phase motor

$R_s$  is the stator resistance

$X_s$  is the stator reactance

$X_r$  is the rotor reactance

$R_r$  is the rotor resistance

$X_m$  is the magnetizing reactance

$Z_f$ , the forward impedance, is a parallel combination of  $0.5X_m$  and  $0.5R_r/s$ . Therefore expressing  $Z_f$  as  $R_f + jX_f$ , gives:

$$R_f = \frac{\left(\frac{X_m}{2}\right)^2}{s \frac{\left(X_r + \frac{X_m}{2}\right)^2}{R_r} + \frac{R_r}{s}} \quad (17)$$

Similarly  $Z_b$ , the backward impedance, is a parallel combination of  $0.5X_m$  and  $0.5R_r/(2-s)$ , there for the real part  $R_b$  of  $Z_b = R_b + jX_b$  is given as:

$$R_b = \frac{\left(\frac{X_m}{2}\right)^2}{(2-s)\frac{\left(X_r + \frac{X_m}{2}\right)^2}{R_r} + \frac{R_r}{2-s}} \quad (18)$$

As outlined in Fitzgerald et al [16], the mechanical power and torque can be computed by application of the equations developed for the polyphase motor as described in chapter 9. The forward and backward power are calculated as follows:

$$P_f = I_s^2 0.5 R_f \quad (19)$$

Where  $R_f$  is as given in equation (17). And the torque is

$$T_f = \frac{P_f}{\omega_s} \quad (20)$$

Similarly, the backward power is given by

$$P_b = I_s^2 0.5 R_b \quad (21)$$

Where  $R_b$  is as given in equation (10). The torque is

$$T_b = \frac{P_b}{\omega_s} \quad (22)$$

The resulting mechanical torque for a single phase induction motor is therefore given by

$$T = T_f - T_b \quad (23)$$

## 2.5 Power System Stability

### 2.5.1 Steady State Stability Analysis

Steady state analysis examines the stability of a system under small incremental variations in parameters and operating conditions about a steady state operating condition (Grainger and Stevenson [4]). The system equations are linearized and solved by methods of linear analysis to determine the steady state stability. The stability analysis of a system in steady state is done using the synchronizing power coefficient as described in section 5.4 of Machowski et al [5]. The requirement for stability is such that the derivative of the Power Angle characteristic, or  $K_E$ , is such that:

$$K_{E_q} > 0 \quad (24)$$

Where  $K_{E'}$  is given by:

$$K_{E'} = \frac{E_q' V_s}{x_d'} \cos \delta + \frac{V_s^2}{2} \frac{x_d' - x_q'}{x_d' x_q'} \cos 2\delta \quad (25)$$

It is also necessary to check for the rotor dynamics by using the transient synchronizing power coefficient.

$$K_{E_q'} > K_{E_q} \quad (26)$$

The use of eigenvalues is a technique to determine stability of a linearized model. This is described in section 5.4 of Machowski et al [5].

$$\lambda_{1,2} = -\frac{D}{4H} \pm \sqrt{\left(\frac{D}{4H}\right)^2 - \frac{K_{E_q'} \times 100\pi}{2H}} \quad (27)$$

D is the damping coefficient given by equation (5.24) in Machowski et al [5] but is simplified in Power System Stability lecture notes [22] and quoted by Steiner [24] as:

$$D = V_s^2 \left[ \frac{(X_d' - X_d'')}{x_d'^2} T_{d0}'' \sin^2 \delta + \frac{(X_q' - X_q'')}{x_q'^2} T_{q0}'' \cos^2 \delta \right] \times 2\pi f \quad (28)$$

The equation 26 for damping is discussed further in section 3.2 of this thesis. The other factor used for assessment of stability is the damping ratio which is calculated as follows:

$$\xi = \frac{D}{2\sqrt{2HK_{E'} 2\pi f}} \quad (29)$$

The damping ratio can also be calculated from the Eigen values of a system as follows:

$$\xi = \frac{-\text{Real}(\lambda)}{|\lambda|} \quad (30)$$

### 2.5.2 Transient Stability Analysis

Transient stability involves large system disturbances like an open conductor fault. One of the techniques used for determination of stability in this case is the equal area criterion as described in sections 5.4.3 and 6.1 of Machowski et al [5] and in chapter 4 of Kimbark [8]. The reason for the use of this method is because the magnitude of the

disturbance does not allow for linearization. The non-linearity of the equation of motion must be retained.

The method provides the means of finding the maximum angle of swing. It provides a simple indication of whether synchronism can be maintained and a rough measure of the margin of stability [16]. The method can be exemplified by considering a power angle curve as shown below.

The figure below show graphs of the power angle characteristic curve. Curve 1 shows the pre-fault situation and curve 2 is the curve for the system with an open conductor fault. From the characteristic equation:

$$P_e = \frac{E_q V_s}{x'_d} \sin \delta + \frac{V_s^2}{2} \frac{x'_d - x'_q}{x'_d x'_q} \sin 2\delta \quad (31)$$

Where  $x'_d$  and  $x'_q$  describe the line reactances, it has been shown using symmetrical components that the open conductor reactances are larger by an effective reactance from the negative and zero sequence circuits. Thus the amplitude of the open conductor curve is reduced. With an assumed constant mechanical input, the new steady state power angle becomes  $\delta_b$ .

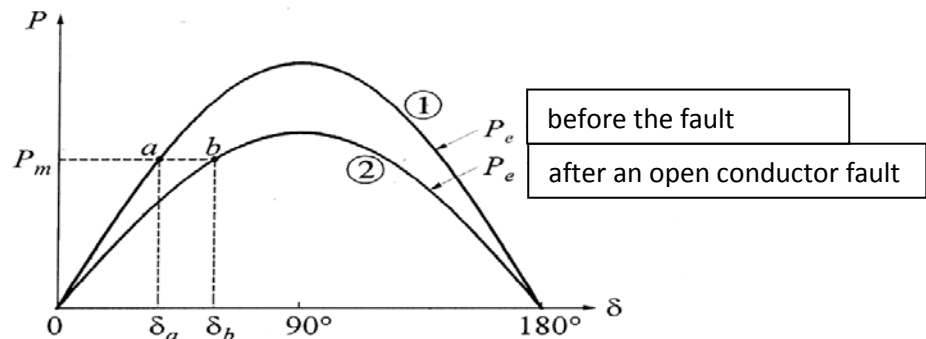


**Figure 9: Power angle characteristic curves for a system before and after a fault.**

The equal area criterion can be exemplified by analysis of the response to a step change in  $P_m$  as demonstrated by Kundur [18]. Increasing the input from  $P_{m0}$  to  $P_{m1}$ , increases the power angle from  $\delta_0$  to  $\delta_1$ . The area A1, between  $P_{m1}$  and the characteristic curve

between the angles, is called the accelerating area. In order to ensure stability, an equivalent amount of area  $A_2$  is required to decelerate the machine.

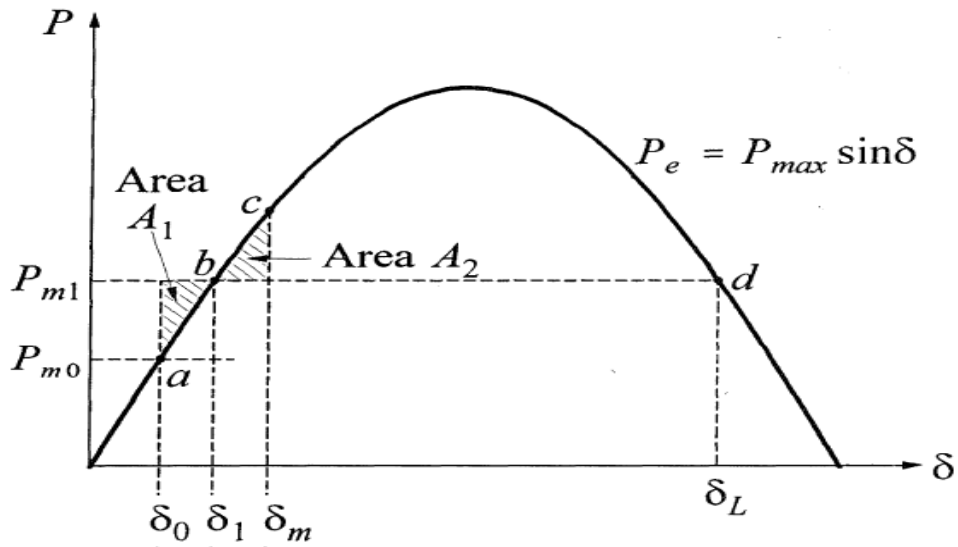


Figure 10: Illustration of the equal area criterion after a change in mechanical input

The stability analysis using the equal area criterion is applied to the open conductor case in chapter 6 of this thesis.

### 3. Damping

One of the important aspects of stability of a power system is the damping of the system. As such, it was necessary to understand how the damping of a system is affected during an open conductor fault. This chapter outlines the aspects of damping which were investigated and the references from which the information was acquired.

#### 3.1 Power System Network Description

A standard network of a synchronous machine connected to an infinite grid through an external circuit of a transformer and a short line was used for illustrative and demonstrative purposes during the development of the damping equations. The equations can be extended to any circuit. A circuit is as shown below:

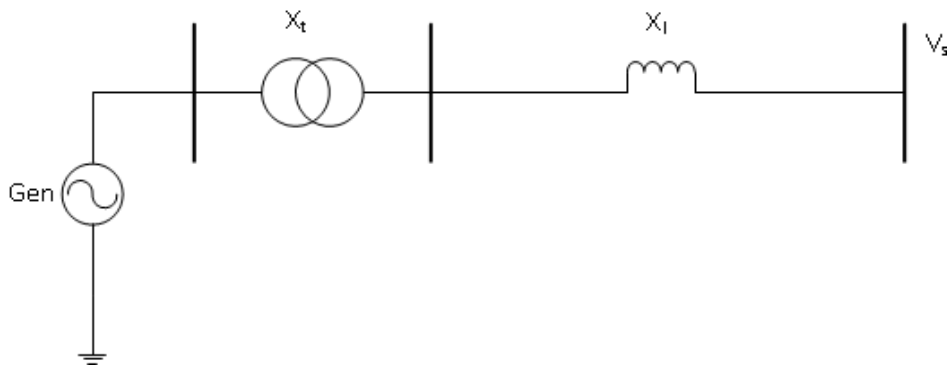


**Figure 11: Synchronous Machine connected to an infinite grid through a transformer and line.**

- Where:
- $X_l$  is the line reactance
  - $X_t$  is the transformer reactance
  - $V_s$  is the voltage of the infinite grid
  - Gen is the synchronous generator

The resistance of the line and transformer has been neglected.



## 3.2 Positive Damping

The derivation of positive damping equation is outlined in Machowski at el [5], Kimbark [9] and Crary [15]. In all these references, it is stated that the derivation of the equation is based on papers by R.H. Park [10] and [11] written in 1929 and 1933 respectively. R. H. Park also makes reference to R. E. Doherty and C. A. Nickle [12] written in 1927. The positive damping equation is also quoted by O.G.C Dahl [13]. In Dahl, however, it is stated that the damping formula in [12] is for small sinusoidal low frequency oscillations about a mean displacement angle. In Park, the equations for damping are for any condition of slip and any number of rotor circuits.

A different approach in the derivation of the positive damping has been outlined by Liwschitz [14]. It is based on the simple physical explanation that the positive damping is dependent on the primary voltage and secondary resistance.

This thesis seeks to outline the applicability of these equations on the open conductor fault situation.

### 3.2.1 Positive Damping Equation

Damping in synchronous machines is an asynchronous effect and as such, the derivation of the formula is based on the induction machine theory. Positive damping is considered linear for small slips and is considered to be directly proportional to the slip (Chapter XIX in Dahl [13]). It is dependent on the voltage impressed on the external circuit.

In the derivation of the formula, the following assumptions are made.

1. The resistances of both the armature and field winding
2. Damping is only produced by the damper windings
3. Small slip
4. Principal damping produced by one set or rotor damper windings only

The equivalent circuit is as follows:

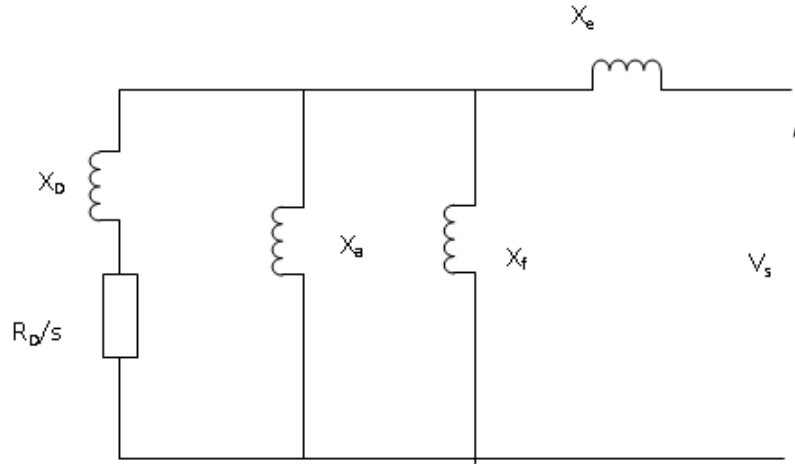


**Figure 12: Equivalent circuit of a synchronous machine operating as an induction machine.**

Where:  $R_D$  is the resistance of the damper windings

$X_D$  is the reactance of the damper windings

$X_a$  is the armature reactance

$X_f$  is the field reactance

$X_e$  is the external reactance due to the transformer and the transmission line

The equation for the damping power is:

$$P_D = V_s^2 \left( \frac{X'_d - X''_d}{(X_{eq} + X'_d)^2} \frac{X'_d}{X''_d} T_d'' \sin^2 \delta + \frac{X'_q - X''_q}{(X_{eq} + X'_q)^2} \frac{X'_q}{X''_q} T_q'' \cos^2 \delta \right) \Delta w \quad (32)$$

Where:  $P_D$  is the instantaneous damping power in per unit

$V$  is the infinite bus voltage

$W$  is the rotor speed

$\delta$  is the angle by which the machine leads the infinite bus

$T_d''$  and  $T_q''$  are the subtransient short-circuit time constants

$X'_d, X''_d, X'_q$  and  $X''_q$  are the machine reactances in per unit

$X_{eq}$  is equal to  $X_e$ , the external reactance which is in series with the armature.

### 3.2.2 Application to the Open Conductor Case

As explained in section 2.1.1 of this thesis, the open conductor is resolved in to symmetrical components and positive, negative and zero sequence networks connected in parallel. Thus, the effect on the positive sequence network, is an introduction of an impedance representing the parallel connection of the negative and zero sequence networks as explained in chapter VI of Kimbark [8]. The circuit to be considered during an open conductor case is therefore, with an extra effective impedance  $X_{eff}$  at the point of fault as shown below:

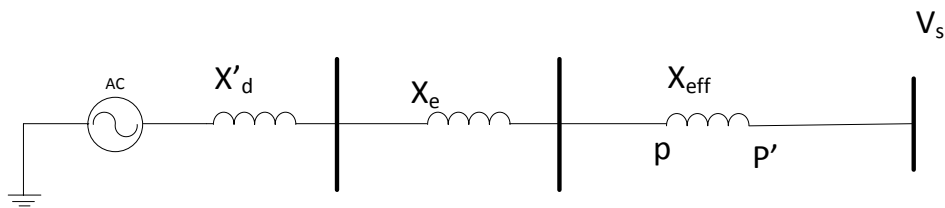


**Figure 13: Equivalent circuit of a synchronous machine during open conductor fault**

Where:  $V$  is the infinite bus voltage

$X_e$  is the external reactance which is in series with the armature.

$X_d'$  is the machine transient reactance in per unit

$X_{eff}$  is the reactance calculated from the parallel connection of the negative and zero sequence circuits as explained in section 2.1.1

The  $X_{eq}$  in equation 30 becomes the sum of  $X_e$  and  $X_{eff}$

### 3.2.3 Application to the Two Open Conductor Case

In the case of this type of fault, the connection of the sequence networks is as explained in section 2.1.2 of this thesis. Therefore the effective reactance  $X_{eff}$  to be inserted in to the positive sequence network is a series connection of the negative and zero sequence impedances.

### 3.3 Negative Damping

Two approaches were identified for the derivation of the equation for the negative damping. The first approach is outlined in chapter XIV of Kimbark [8], chapter XIX of Dahl [13] and chapter 6 of Crary [15]. The equation is quoted in section 13.4.5 of Kundur [18]. This approach can be referred to as the Induction Machine Concept and the equation is derived similar to the positive damping. The second approach is outlined in Fitzgerald et al [16] and Hindmarsh et al [17]. This approach is based on the Single Phase Operation Concept.

#### 3.3.1 Negative Damping Equation: Symmetrical Components Concept

An asymmetrical fault will produce negative sequence currents that will flow in the generator. These currents will produce an mmf across the air gap traveling at synchronous speed with respect to the stator but in the opposite direction of rotation from that of the rotor [15]. Therefore the slip, with respect to the rotor, is twice normal frequency. The torque produced due to this negative phase sequence flux is subsequently in the direction opposite to that of the rotation of the rotor and always acts to decelerate the rotor. It is thus referred to as the braking or retarding torque. The representation of this is as shown in an equivalent circuit below.

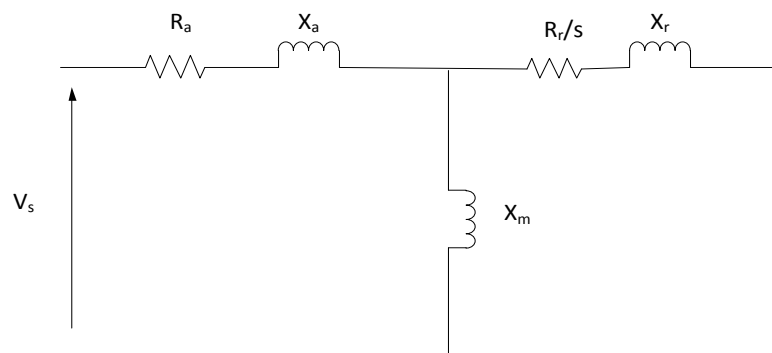


**Figure 14: Equivalent circuit of a synchronous machine operating as an induction machine**

- Where:
- $R_a$  is the armature resistance
  - $V_s$  is the infinite grid voltage
  - $X_a$  is the armature reactance
  - $X_m$  is the magnetizing reactance
  - $R_r$  is the rotor resistance
  - $X_r$  is the rotor reactance

Reducing the impedances to a Thevinin equivalent across the voltage gives negative sequence impedance  $Z^-$  as follows:

$$Z^- = R_a + jX_a + \frac{(R_r / s + jX_r)jX_m}{R_r / s + j(X_r + X_m)} \quad (33)$$

$$Z^- = R_a + \frac{(R_r / s)X_m^2}{(R_r / s)^2 + (X_r + X_m)^2} + j \left( X_a + \frac{X_m [(R_r / s)^2 + X_r(X_r + X_m)]}{(R_r / s)^2 + (X_r + X_m)^2} \right) \quad (34)$$

Therefore the negative sequence resistance is

$$R^- = R_a + \frac{(R_r / s)X_m^2}{(R_r / s)^2 + (X_r + X_m)^2} \quad (35)$$

When the magnetizing reactance  $X_m$  is neglected ( $X_m$  equal to infinity), the negative resistance becomes:

$$R^- = R_a + \frac{R_r}{s} \quad (36)$$

The negative sequence slip can be approximated to 2 with minimal error, this gives

$$R^- = R_a + \frac{R_r}{2} \quad (37)$$

Therefore the rotor resistance  $R_r$  can be expressed as:

$$R_r = 2[R^- - R_a] \quad (38)$$

Thus the effective damper resistance at double frequency is twice the difference between the negative sequence and positive sequence resistances of the synchronous machine [13].

The negative phase resistance can be determined by the test explained in section 2.3 of this thesis.

Finally, the damping power is given as

$$P^- = I_2^2 R_r \frac{1-s}{s} \quad (39)$$

Inserting equation 38 and slip  $s = 2$  in to equation 39 gives the negative damping power as:

$$P^- = -I_2^2 (R^- - R_a) \quad (40)$$

### 3.3.2 Negative Damping Equation: Single Phasing Concept

A condition where a 3 phase induction machine is operating with one of the stator phases open circuited is referred to as single phasing (as explained in section 6.11.3 project 3 of Chee-Mun Ong [19]).

Using the theory of single phase motors outlined in section 2.4 of this thesis, the equivalent circuit is represented as follows:

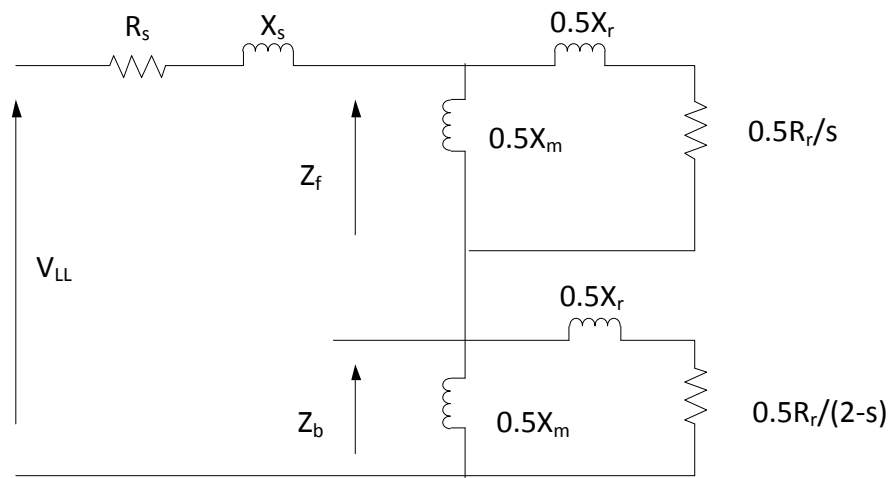


Figure 15: Equivalent circuit of a 3 phase induction machine with one terminal open circuited

Where:  $V_{LL}$  is the line to line voltage

$Z_f$  is the forward impedance due to forward rotating flux

$Z_b$  is the backward impedance due to reverse rotating flux

Of interest in the calculation of the negative damping power is the backward impedance which is in parallel with the magnetizing reactance as follows:

$$Z_b = \frac{R_r}{2-s} + jX_r \parallel j\frac{X_m}{2} \quad (41)$$

Expressing the backward impedance as a real and imaginary part, we have:

$$Z_b = R_b + jX_b \quad (42)$$

Where:

$$R_b = \frac{\left(\frac{X_m}{2}\right)^2}{(2-s)\frac{\left(X_r + \frac{X_m}{2}\right)^2}{R_r} + \frac{R_r}{2-s}} \quad (43)$$

Negative damping power is therefore given as

$$P_b = I_s^2 R_b \quad (44)$$

Where  $R_b$  is as given in equation (23) and  $I_s$  is the line current in phases **b** and **c** when **a** is the open conductor phase.

### 3.4 Discussion

Section 3.2 outlined the equation for positive damping and how it can be applied to cases involving one and two open conductor faults. Similarly, section 3.3 outlined the equation for negative damping. The subsequent chapters in this thesis will look at specific cases and use these equations to calculate damping coefficients and ratios for specific power systems.

## 4. Power Angle Characteristic Curve of the Synchronous Generator – Case Study

The objective in this case study was to draw the Power Angle characteristic curve for the steady state and transient situations for the network shown below. The network that was used is a synchronous generator directly connected to the grid as shown in the figure below.

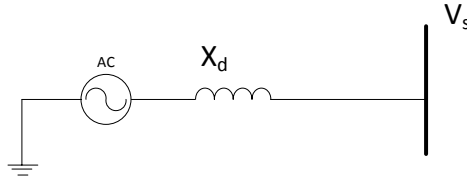


Figure 16: Equivalent circuit of synchronous machine connected to an infinite grid through a line.

In this case, the type of synchronous machine used was the salient pole machine. A detailed account of synchronous machine parameters is as shown in appendix A.

A summary of machine parameters for the salient pole are as shown below.

$$\begin{array}{lll} X_d = 1.05 & X_q = 0.66 & X_q'' = 0.25 \\ X'd = 0.33 & X''d = 0.25 & \\ T'd0 = 2.49 & T''d0 = 0.06 & T''q0 = 0.15 \end{array}$$

The voltage at the infinite grid was set at 1 pu

### 4.1 Analytically

Analytically, this was derived using Matlab. The initial load of the generator was 0.8-j0.6 pu. The Matlab file used in the calculations is attached in Appendix J. However, the basic equation used for the derivation of the curve is equation (30) in chapter 3 of this thesis.

$$P_D = V_s^2 \left( \frac{X'_d - X''_d}{(X_{eq} + X'_d)^2} \frac{X'_d}{X''_d} T''_d \sin^2 \delta + \frac{X'_q - X''_q}{(X_{eq} + X'_q)^2} \frac{X'_q}{X''_q} T''_q \cos^2 \delta \right) \Delta w \quad (28)$$

Since the synchronous machine is connected directly,  $X_{eq} = 0$ .



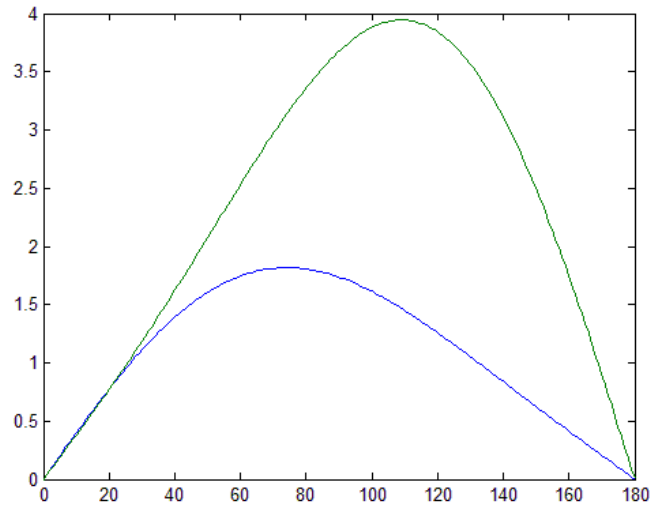


Figure 17: Power angle characteristic curve for steady state (blue) and transient (green) conditions.

## 4.2 Using SIMPOW

From the network above, a power flow and dynamic file was set up in SIMPOW. These files are as shown in appendix B. In the dynamic file, a table was set up to varying the turbine input to the synchronous generator from 0 to 1 pu over a period of 100 seconds. The curve of power against angle was drawn as shown below:

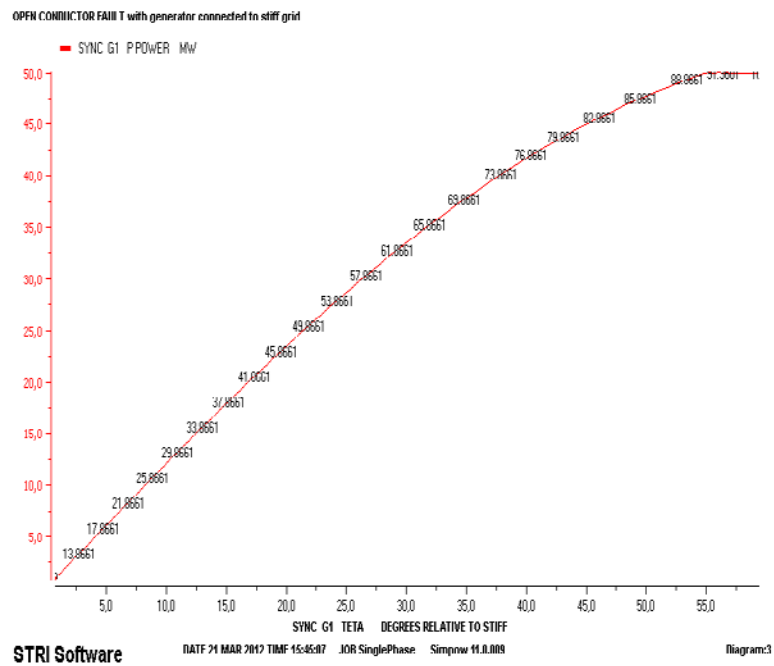


Figure 18: Power angle characteristic curve using simpow.

For different amounts of reactive power, and with and without voltage regulation, several cases were simulated and power angle curves were drawn. The curves for the other cases are shown in appendix K.

### 4.3 Discussion

The power angle curve using analytical means was perfectly drawn for power angles from zero to  $180^\circ$ . This was done using the steady state system parameters as well as using the transient parameters. However, the use of SIMPOW to draw this curve proved to be a challenge. First, the curve was dependent on the rate of change of the turbine input. The turbine input was used to vary the power generation of the machine. Secondly, the curve could only be drawn for a limited range of power angle. For the 8 cases that were conducted, it was not possible to draw the curve beyond  $60^\circ$ .

Consequently, the power angle curves that were drawn for the open conductor cases discussed in the succeeding chapters were drawn using Matlab instead of SIMPOW.

## 5. Damping Coefficient - Case Studies

Six cases were considered. These cases were solved both analytically and also using simulations with SIMPOW. In the simulation, two types of synchronous machines were used. Type 4 is a Voltage-Behind Reactance (VBR) model and damping has to be explicitly defined through the definition of the parameter  $D$ . The Type 2A synchronous machine has damper windings in the d-axis and the damping is thus already included in the model. The network which was used for all cases is as shown below.

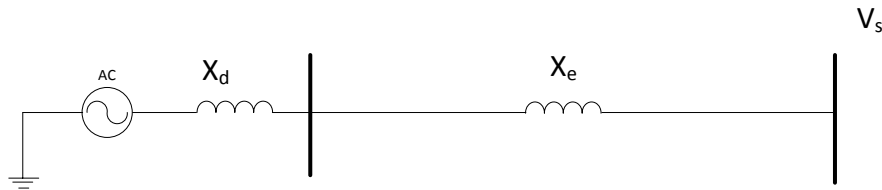


Figure 19: Equivalent circuit of a synchronous machine connected to the grid

### 5.1 Description of the case studies

Using a voltage base of 10KV and Power base of 50MVA, the base impedance for the transmission line was taken as 2 ohms. This was used to calculate the values in pu for analytic calculations. However, in SIMPOW the line was declared as type 1 and values defines as ohms per unit length.

#### Case 1: Synchronous Machine directly connected to Infinite grid

In this case a synchronous machine was directly connected to the infinite grid with no transformer or transmission line in between. This was modeled in the calculations and simulations by assigning zero reactance to the line.

#### Case 2: As in case 1 but with open conductor in phase A

This was solved analytically using the symmetrical components tool as explained in chapter 2 of this thesis. The network was resolved in to sequence networks and then the parallel connection of the negative and zero sequence networks was resolved to provide an effective reactance which was introduced in to the positive sequence network and used for calculations.

In the simulation, the open conductor was modeled by a circuit breaker which opened on single pole switching in phase A.

### Case 3: Synchronous Machine connected to Infinite grid through transmission line

In this case a synchronous machine was connected to the grid through a transmission line with a reactance of 0.001 pu.

### Case 4: Synchronous Machine connected to Infinite grid through transmission line

This case is the same as case 3 but for a transmission line with a reactance of 0.1 pu.

### Case 5: Synchronous Machine connected to Infinite grid through transmission line

This case is the same as case 3 but for a transmission line with a reactance of 0.2 pu.

### Case 6: Synchronous Machine connected to Infinite grid through transmission line

This case is the same as case 3 but for a transmission line with a reactance of 0.4 pu.

### Case 7: Same as case 6 but with an OCF

In this case a synchronous machine was connected to the grid through a transmission line with a reactance of 0.4 pu and an open conductor fault in one phase.

## 5.2 Calculation of Damping Coefficient - Analytically

The following parameters were calculated using the formulae below.

a) Damping constant using the formula:

$$D = V_s^2 \left( \frac{X_d' - X_d''}{(X_{eq} + X_d')^2} T_{d0}'' \sin^2 \delta + \frac{X_q' - X_q''}{(X_{eq} + X_q')^2} T_{q0}'' \cos^2 \delta \right) \times 2\pi f \quad (45)$$

b) Transient Synchronizing constant,  $K_{E'}$

$$K_{E'} = \frac{E_q' V_s}{x_d'} \cos \delta + \frac{V_s^2}{2} \frac{x_d' - x_q'}{x_d' x_q'} \cos 2\delta \quad (46)$$

c) Eigen Values  $\lambda$

$$\lambda_{1,2} = -\frac{D}{4H} \pm \sqrt{\left(\frac{D}{4H}\right)^2 - \frac{K_{E_q} \times 100\pi}{2H}} \quad (47)$$

Damping ratio

$$\xi = \frac{D}{2\sqrt{2HK_{E_q} \cdot 2\pi f}} \quad (48)$$

d) Negative Sequence Damping,  $P^-$

This was calculated using the formulae given as:

$$P^- = -I_2^2 (R^- - R_a) \quad (49)$$

Where  $I_2$  is the negative sequence current in the negative sequence circuit.

The results obtained from the calculations are as shown in the table below

Cases (reactance in pu)	D (Damping Coefficient)	$K_E$ (Synchronising Coefficient)	Eigen Values ( $\lambda$ )	$P^-$ (Negative Sequence Power)	$\xi$ (Damping Ratio)
Case 1 - No line	40.5	2.3	-3.2691+j1.6394	0	30.25
Case 2 - OCF	34.8	2.07	-2.8095+j1.5679	3.28	27.4
Case 3 - Line with 0.001	40.4	2.3	-3.258+j1.6388	0	30.17
Case 4 - Line with 0.1	29.7	2.1	-2.395+j1.583	0	23.4
Case 5 - Line with 0.2	22.6	1.9	-1.821+j1.5288	0	18.6
Case 6 - Line with 0.4	14.2	1.6	-1.141+j1.4366	0	12.5
Case 7- Line with 0.4 and OCF	12.9	1.5	-1.039+j1.396		11.7

### 5.3 Using a Type 4 Synchronous Generator model in SIMPOW

The SIMPOW files were set up as shown in Appendix D. The calculated value of the damping coefficient was used in the DYNPOW file to represent the damping of the machine. From the simulation, linear analysis was performed to obtain the eigen values which were used to calculate the damping ratio. The damping ratio is given by the formula stated in section 2.5 and repeated here:

$$\xi = \frac{-\text{Real}(\lambda)}{|\lambda|} \quad (30)$$

The results obtained are represented in the table shown below.

Cases (reactance in pu)	Eigen Values ( $\lambda$ )	Damping ratio ( $\xi$ )
Case 1 (No Line), D=40.5	-3.269+-j1.639	30.2
Case 2 OCF (No Line), D=34.8	-2.8065+-j1.661	25.97
Case 3 with line ( $x=0.001$ )	-3.258+-j1.6399	30.1
Case 4 with line ( $x=0.1$ )	-2.395+-j1.611	23.0
Case 5 with line ( $x=0.2$ )	-1.8226+-j1.571	18.2
Case 6 with line ( $x=0.4$ )	-1.1452+-j1.484	12.1
Case 7 with line ( $x=0.4$ ) - OCF	-1.04+-j1.486	11.1

### 5.4 Using a Type 2A Synchronous Generator model in SIMPOW

The SIMPOW files were set up as shown in Appendix D. The model used has d-axis windings already defined. From the simulation, linear analysis was performed to obtain the Eigen values which were used to calculate the damping ratio according to the formula in equation (28). The results are represented in the table shown below.

Cases (reactance in pu)	Eigen Values ( $\lambda$ )	Damping ratio ( $\xi$ ) [ %]
Case 1 (No Line)	-2.667+-j2.019	20.6
Case 2 - OCF	-1.980+-j1.874	16.6
Case 3 with line ( $x=0.001$ )	-2.33+-j2.0069	18.2
Case 4 with line ( $x=0.1$ )	-1.871+-j1.895	15.5
Case 5 with line ( $x=0.2$ )	-1.463+-j1.827	14.1
Case 6 with line ( $x=0.4$ )	-1.1136+-j1.643	10.7
Case 7 with line ( $x=0.4$ ) - OCF	-0.4193+-1.1975	5.6

The simulation curve shown below is for case 7 (With a line of reactance 0.4 ohms). It shows a for power flow from the generator to the infinite grid through a line with an open conductor fault.

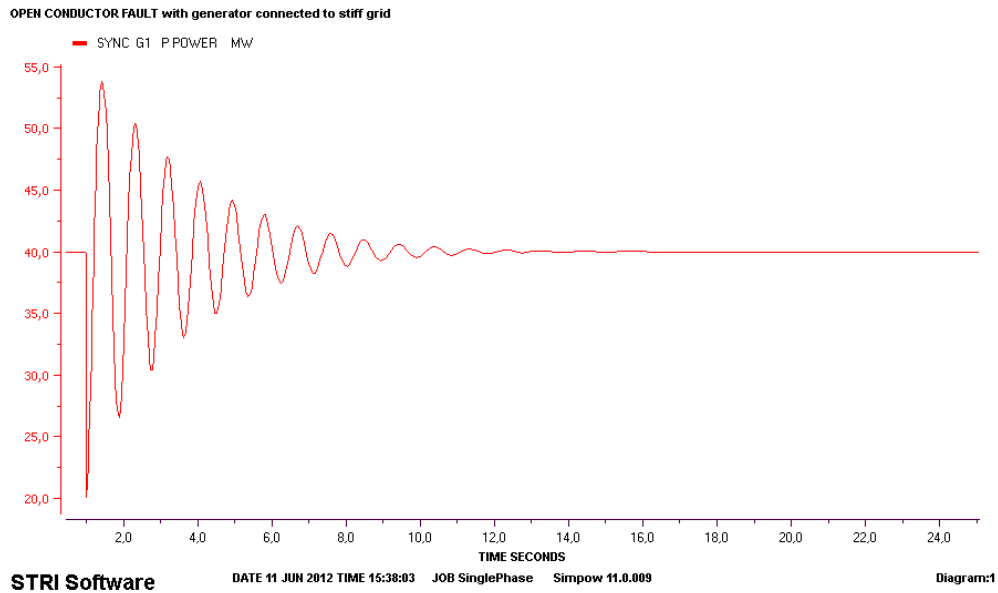


**Figure 20: Equivalent circuit of a synchronous machine connected to the grid**

## 5.5 Discussion

The idea behind the use of the three methods outlined in this chapter was to use the equations discussed in chapter 3 to calculate analytically the parameters of a specific case, and then confirm the results using simulation of a model using a simple machine model (Type 4), whose damping has to be explicitly defined, and a more complicated model (Type 2A) with inbuilt damping. This would have proved that the discussed equations in chapter 3 can be applied for open conductor cases as proposed.

The results obtained analytically were very close to the simulation results of Type 4 synchronous machine. However, they were different from the simulation results of a Type 2A machine. For higher values of line reactances, however, the damping ratios were close. For instance, in case 6 which had a line reactance of 0.4 pu, the damping ratios for the three methods were 12.5, 12.1 and 10.7 respectively.

## 6. Transient Stability: Case studies

A case study was conducted to in order to exemplify the analytical method to assess the stability of a network during an open conductor fault. The method of Equal Area was used and the results confirmed using SIMPOW simulation software. The network used is a synchronous machine connected to the infinite grid as shown below.

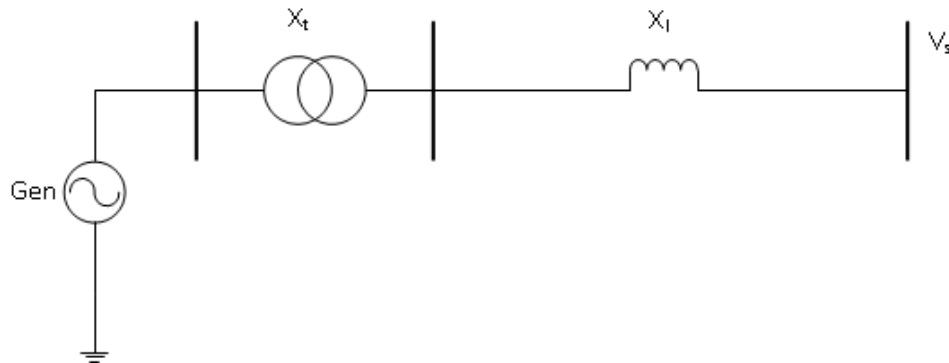


Figure 22: Equivalent circuit of a synchronous machine connected to the grid

The system parameters are outlined as follows:

### Generator:

$X'_d = 0.25$        $X_2 = 0.26$        $X_0 = 1.5$       Earthed through 0.1 reactance

### Transformer

$X_t = 0.1$        $X_2 = 0.1$        $X_0 = 0.5$       Earthed through 0.25 reactance

### Transmission Line

$X_l = 0.1$        $X_2 = 0.1$        $X_0 = 0.5$

Detailed generator parameters are as shown in appendix A.

### 6.1 Analytically

#### Pre Fault situation

For the transient analysis, the circuit was set up and solved on per phase basis as shown below.



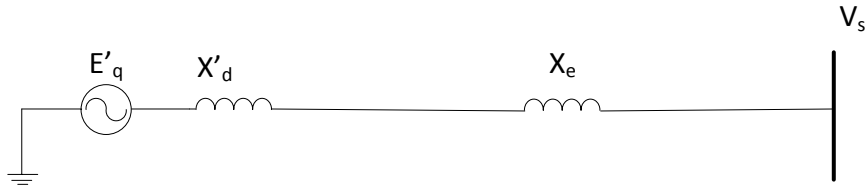


**Figure 23: Equivalent circuit of a synchronous machine connected to the grid**

From the above network, the parameters were calculated as shown below.

$$E'_q = 1.375$$

$$V_s = 1$$

$$x'_d = X'_d + X_e = 0.33 + 0.2 = 0.53$$

$$x'_q = X'_q + X_e = 0.66 + 0.2 = 0.86$$

These were inserted in to the equation below.

$$P_{E'}(\delta) = \frac{E'_q V_s}{x_d} \sin \delta + \frac{V_s^2}{2} \frac{x_d - x_q}{x_d x_q} \sin 2\delta \quad (50)$$

For  $P_{E'}=P_m=0.8$ , the angle  $\delta_1$  was calculated as  $24.4^\circ$ .

### During the Fault

For the open conductor fault situation, the network was resolved in to positive, negative and zero sequence circuits as shown below. The sequence networks are connected in parallel at the point of the open conductor fault.

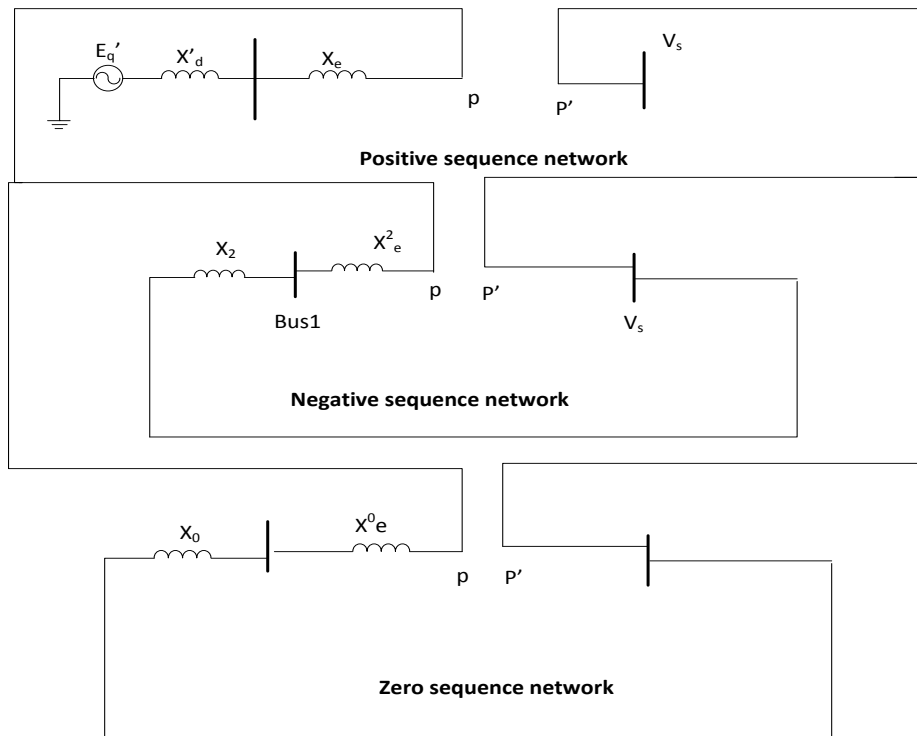


**Figure 24: Connection of sequence networks for an open conductor fault**

The network can be simplified as shown below.

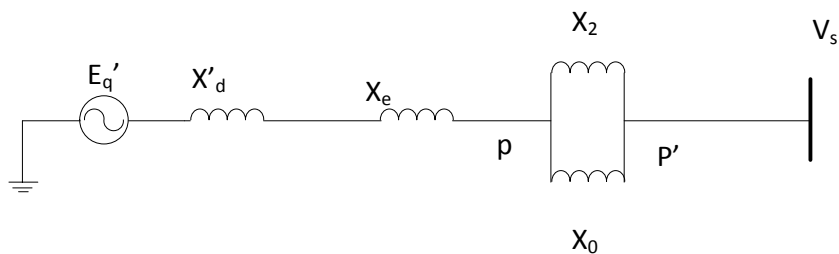


**Figure 25: Addition of the Zero and negative sequence impedances to the positive sequence network**

The parallel connection of the negative and zero sequence reactances was calculated as  $X_{eff}$  and inserted in to the positive sequence network and the final network used for assessment of the open conductor fault is as shown below.

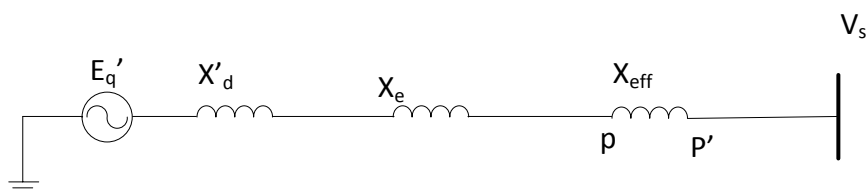


**Figure 26: Equivalent circuit to be used for analysis of an open conductor fault**

Where the parameters are calculated as follows:

$$E'_q = 1.375$$

$$V_s = 1$$

$$x'_d = X'_d + X_e + X_{\text{eff}} = 0.33 + 0.2 + 0.34 = 0.87$$

$$x'_q = X'_q + X_e + X_{\text{eff}} = 0.66 + 0.2 + 0.34 = 1.2$$

Using the equation:

$$P_{E'}(\delta) = \frac{E'_q V_s}{x_d} \sin \delta + \frac{V_s^2}{2} \frac{x_d - x_q}{x_d x_q} \sin 2\delta \quad (51)$$

And inserting  $P_{E'} = 0.8$  gives  $\delta_2$  as  $37.5^\circ$

The power angle curves were obtained for transient case and open conductor cases are as shown below. The red curve is the transient power angle curve, pre-fault curve while the blue curve is the open conductor curve.

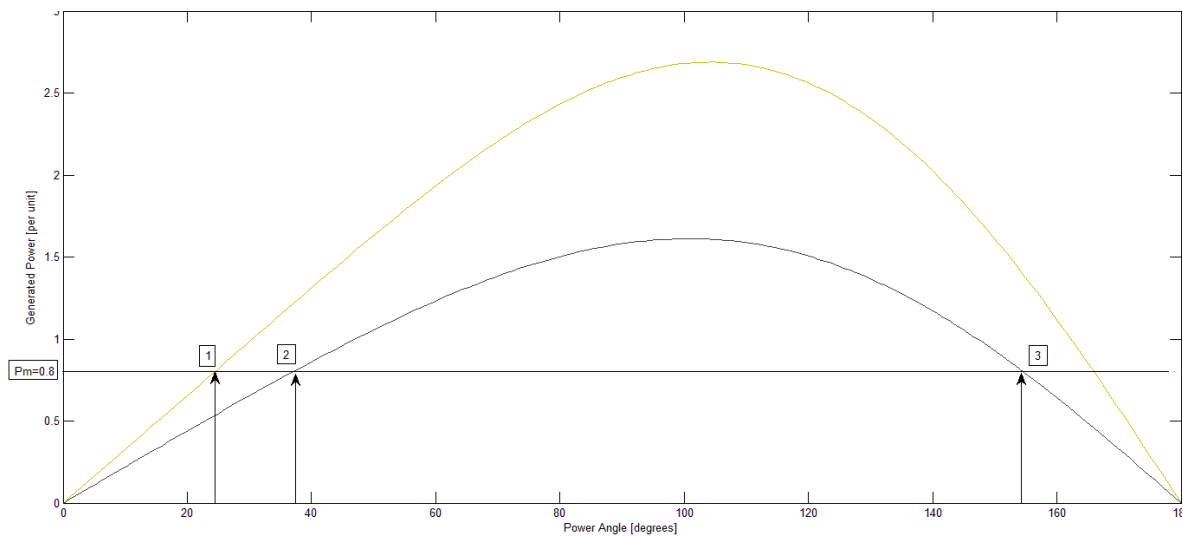


**Figure 27: Power angle characteristic of a system with and without an open conductor fault**

The angles  $\delta_1$ ,  $\delta_2$  and  $\delta_3$  were calculated as  $24.4^\circ$ ,  $37.5^\circ$  and  $152^\circ$

The method of calculating areas between curves is described in chapter 2 of this thesis.

The area between the curves  $P_m=0.8$  and the post fault curve between the angles  $\delta_1$  and  $\delta_2$  was calculated as  $0.183 - 0.122 = 0.061$ .

The area between the curve  $P_m=0.8$  and the post fault curve between angles  $\delta_2$  and  $\delta_3$  was calculated as  $2.602 - 1.599 = 1.043$

Thus, the decelerating area is larger than the acceleration area.

By adjusting the transmission line reactance from 0.1 to 0.8, the power angle curve obtained is as shown below. For the transient curve,

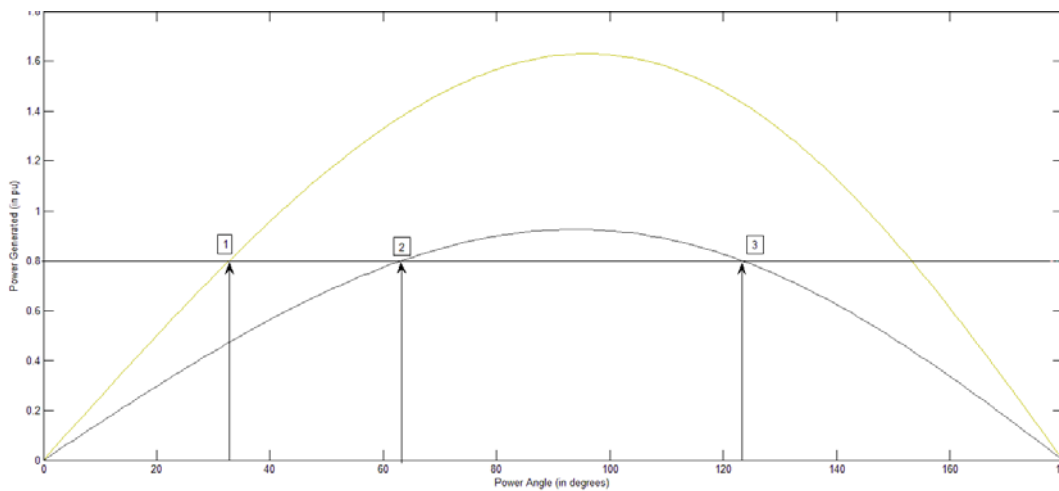


**Figure 28: Power angle characteristic of a system with and without an open conductor fault**

Using the equation below:

$$P_{E'}(\delta) = \frac{E_q' V_s}{x_d} \sin \delta + \frac{V_s^2}{2} \frac{x_d - x_q}{x_d x_q} \sin 2\delta \quad (52)$$

Where, for the transient curve, the parameters are as follows:

$$E_q' = 1.99$$

$$V_s = 1$$

$$x_d' = X_d' + X_e + X_{\text{eff}} = 0.33 + 0.9 = 1.23$$

$$x_q' = X_q' + X_e + X_{\text{eff}} = 0.66 + 0.9 = 1.56$$

and for the post fault parameters:

$$E'_q = 1.99$$

$$V_s = 1$$

$$X'_d = X'_d + X_e + X_{\text{eff}} = 0.33 + 0.9 + 0.93 = 2.16$$

$$X'_q = X'_q + X_e + X_{\text{eff}} = 0.66 + 0.9 + 0.93 = 2.49$$

Equating the above equation to 0.8, we have the angles for  $\delta_1 = 32.8^\circ$ ,  $\delta_2 = 61^\circ$  and  $\delta_3 = 121^\circ$ . Subtracting the area under the post fault curve between  $32.8^\circ$  and  $61^\circ$  from the area under the  $P_m = 0.8$  curve between the same points gives an area of  $0.394 - 0.327 = 0.067$ . Subtracting the area under  $P_m = 0.8$  from the curve between the angles  $61^\circ$  and  $121^\circ$  gives an area of  $1.047 - 1.0008 = 0.0462$

From the two areas it can be seen that accelerating area (0.067) is larger than the deceleration area (0.0462).

## 6.2 SIMPOW simulation results

The OPTPOW and DYNPOW files were set up as shown in appendix E with all the system parameters represented. A summary of some parameters is shown below:

### **OPTPOW File**

#### Transmission Line

$X=0.4$  - reactance per unit length

$L=300$  – Length of transmission line

Using the base power of 50MVA and voltage of 245kV, then line reactance is 0.1 pu

#### Transformer

$EX_{12}=0.1$  – Transformer reactance.

## DYNPOW File

### Synchronous Machine

X2=0.25 - negative sequence reactance

X0=1.5 - zero sequence reactance

### Transformer

CP1=Y CP2=Y – WYE-WYE Winding connection

EX120=0.5 – Zero sequence reactance

RN1=0.001 - Primary earthing through a resistor

RN2=0.0003 – Secondary earthing through a resistor

### Transmission Line

X0=0.5 – Zero sequence reactance

## Results

The result for the dynamic power flow is as shown below. The fault is simulated at 1 second after the start of the program.

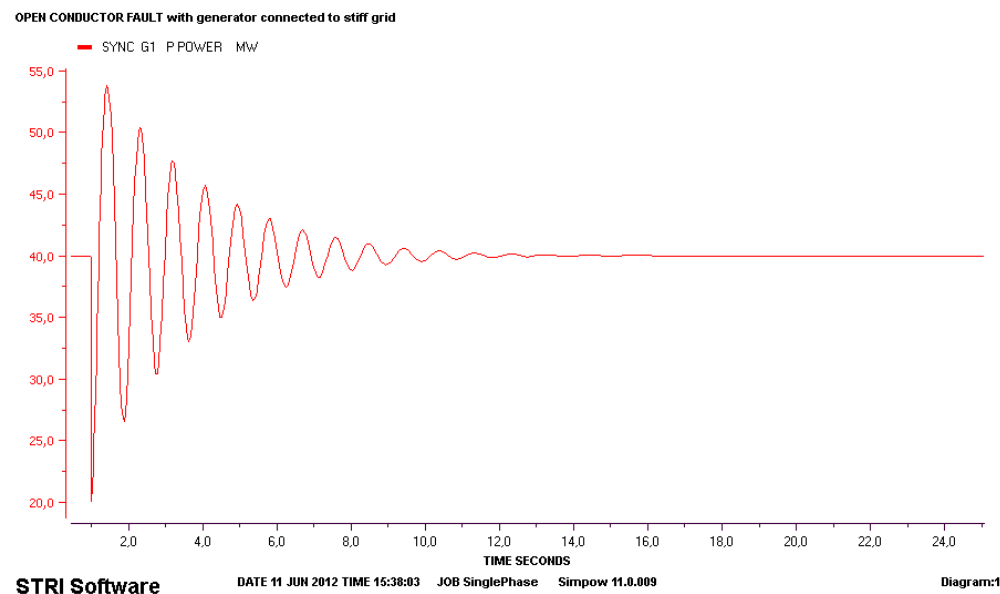


**Figure 29: Power oscillations of the generator after occurrence of a fault**

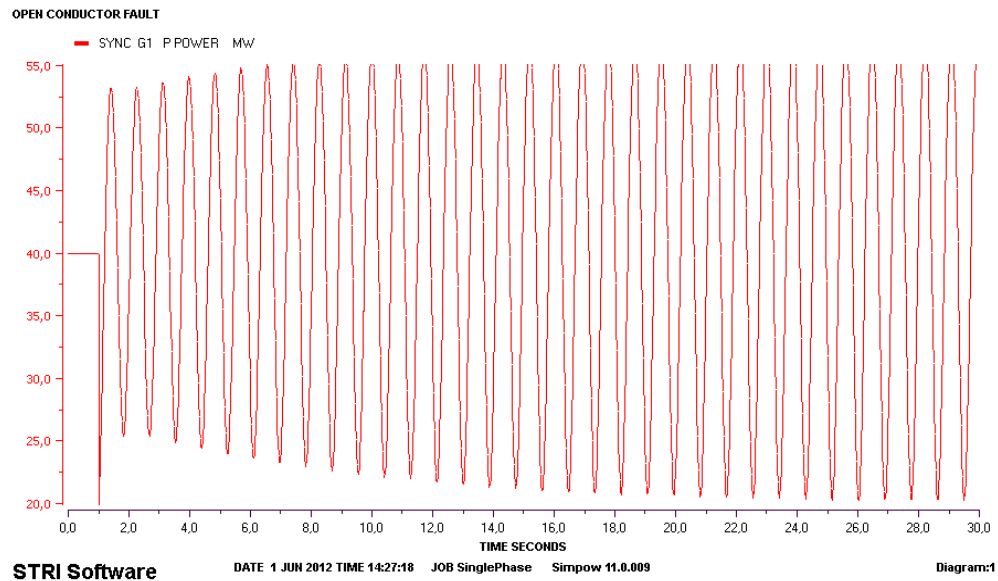


**Figure 30: Power oscillations of the generator after occurrence of a fault**

### 6.3 Discussion

The purpose of in this chapter was to demonstrate the method of transient stability analysis using the Equal Area Criterion and also using SIMPOW simulation.

Using Equal Area criterion, it is easy to see that the figure in 27 is stable compared to the one in figure 28 by comparing the accelerating and decelerating areas of each curve.

In SIMPOW, the first case was simulated and the result is a curve shown in figure 29. The second case result was obtained as shown in figure 30. It shows a curve of power transfer with uncontrollable oscillations after the occurrence of the fault.

## **7. Effect of Power System Grounding and Transformer Winding Configuration: Case Studies**

Two cases were considered in the assessment of the effect of grounding and transformer winding configuration. In the first case, the grounding is adjusted through the adjustment of zero sequence reactances and the dynamic effect observed for the power transfer after the occurrence of the fault. In the second case, the transformer winding configuration was changed and the dynamic effect on the power transfer observed too.

### **7.1 Power System Grounding**

The zero sequence circuit represents the effect of grounding on the power system. For the network presented in chapter 6 of this thesis, the parameters to be considered during grounding of the system are the zero sequence reactance of the synchronous machine and the zero sequence reactance of the transformer.

#### **7.1.1 Analytically**

Adjusting the zero sequence reactance values as follows:

Generator: Reducing  $X_0$  from 1.5 to 0.1 and solidly earthing the neutral.

Transformer: Reducing  $X_{120}$  from 0.5 to 0.1

Both neutrals solidly earthed

The network becomes:



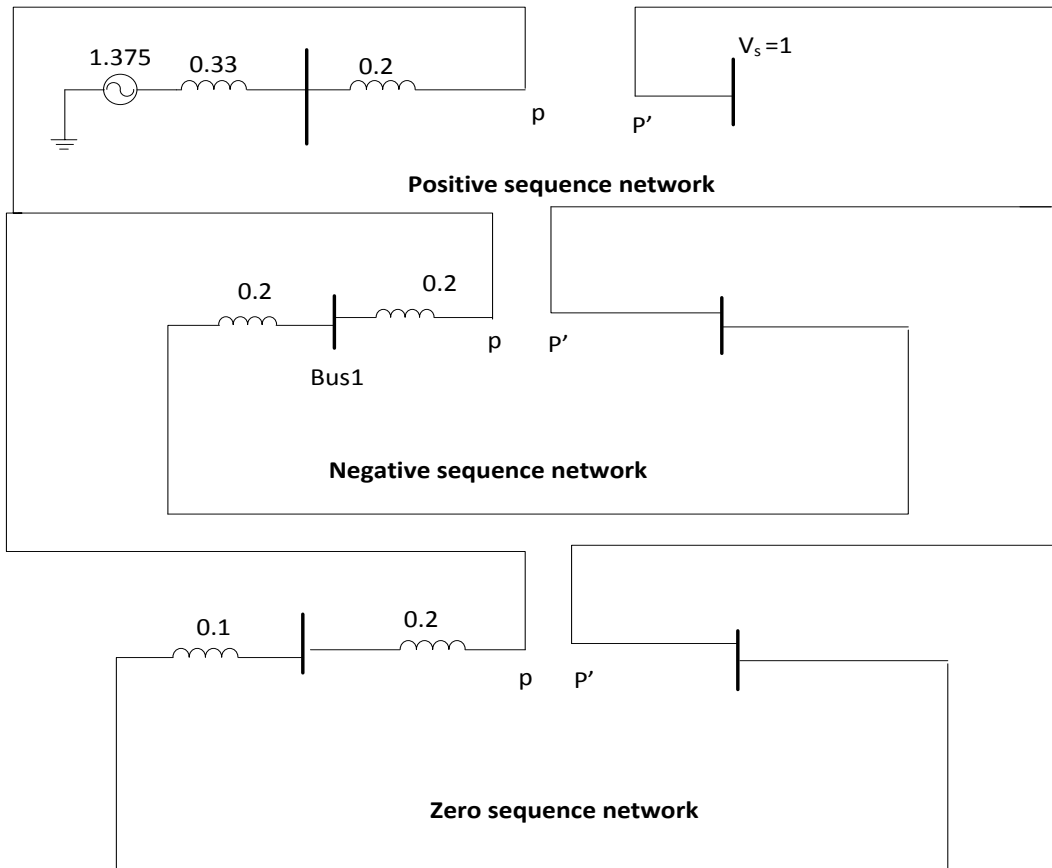


**Figure 31: Connection of sequence networks for an open conductor fault**

The extra impedance to be introduced in the positive circuit becomes the parallel arrangement of 0.3 and 0.4 as shown below.

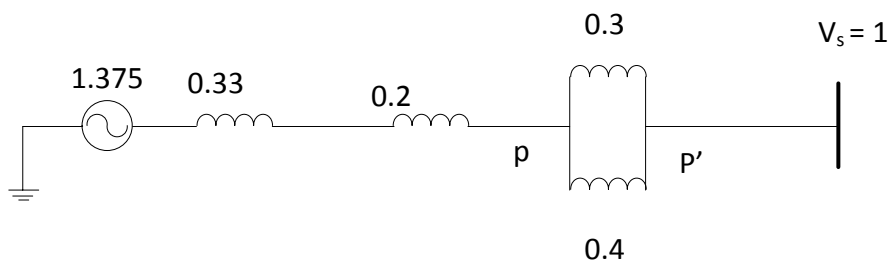


**Figure 32: Addition of the zero and negative sequence impedances to the positive sequence network**

This finally reduces to:

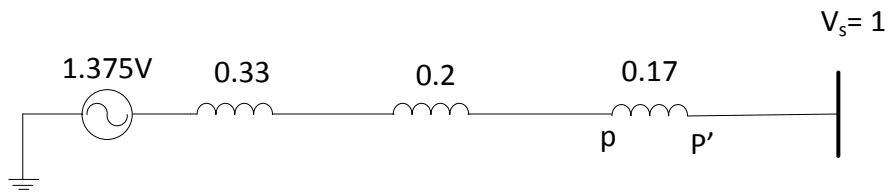


**Figure 33: Equivalent circuit to be used for analysis of an open conductor fault**

Using the parameters in the above circuit, the power angle characteristic for the open conductor case becomes:

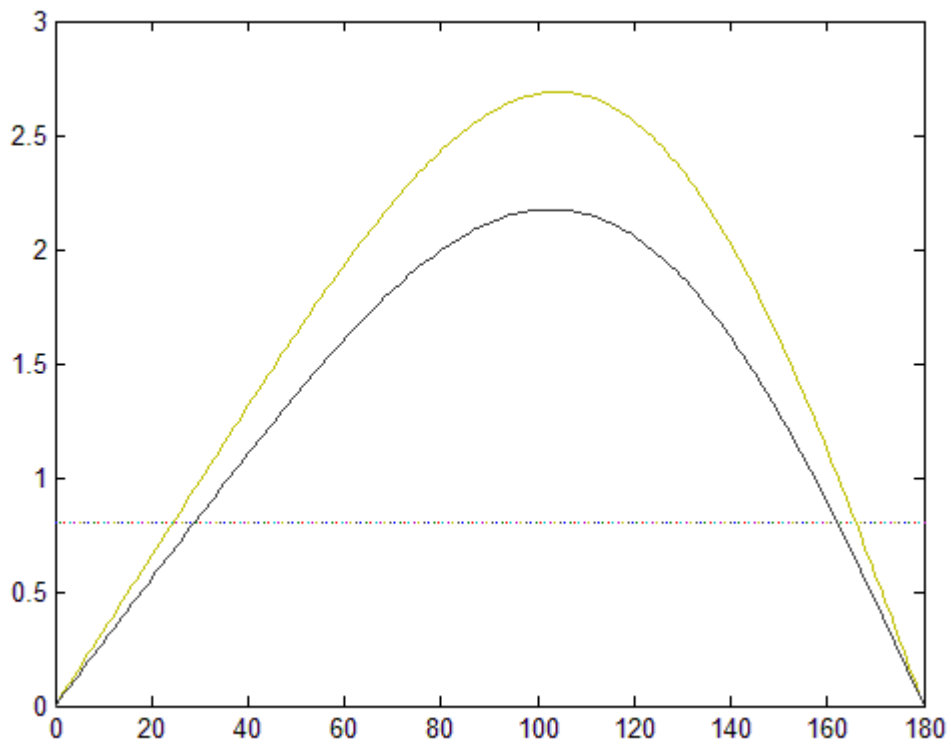


**Figure 34: Power angle characteristic curves for a system before and after the occurrence of the fault**

A visual assessment of the accelerating and decelerating areas clearly shows that the later is much larger.

### 7.1.2 SIMPOW Simulation

Using SIMPOW software, the parameters in the dynamic file DYNPOW were adjusted as follows:

Generator:  $X0 = 0.1$

$R0 = 0$  (Solidly earthed)

Transformer:  $EX120 = 0.1$

$RN1 = 0$  (Primary winding neutral solidly earthed)

$RN2 = 0$  (Secondary winding neutral solidly earthed)

The rest of the parameters are as shown in Appendix F

The results obtained for the dynamic power transfer of power after the occurrence of a fault is shown below.

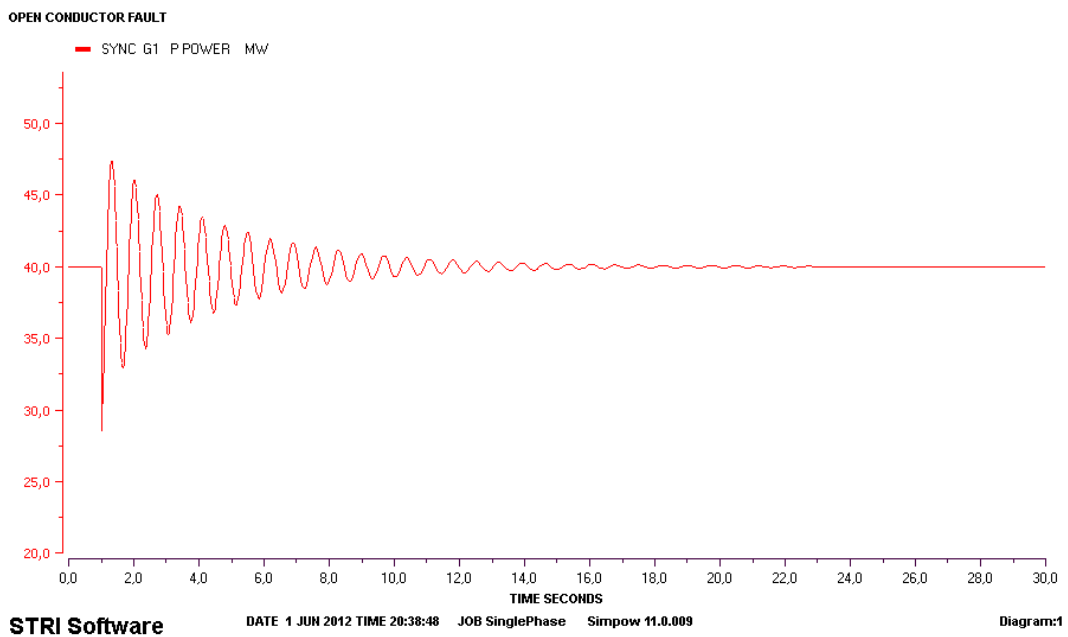


**Figure 35: Power oscillations of the generator after occurrence of a fault**

As can be seen, the synchronous machine returns to the original stable point after the occurrence of the fault after the adjustments made to the zero sequence network.

## 7.2 Transformer Winding Configuration

Instead of adjusting the zero sequence parameters, the network parameters were maintained but the winding configuration was changed to Delta-Wye configuration. The case was solved both analytically and also using SIMPOW software.

### 7.2.1 Analytically

This arrangement eliminates the zero sequence reactance of the synchronous machine. The zero sequence circuit of 0.6 is considered in parallel with the negative sequence circuit calculating the extra impedance to be inserted in to the positive sequence circuit. The circuit becomes:

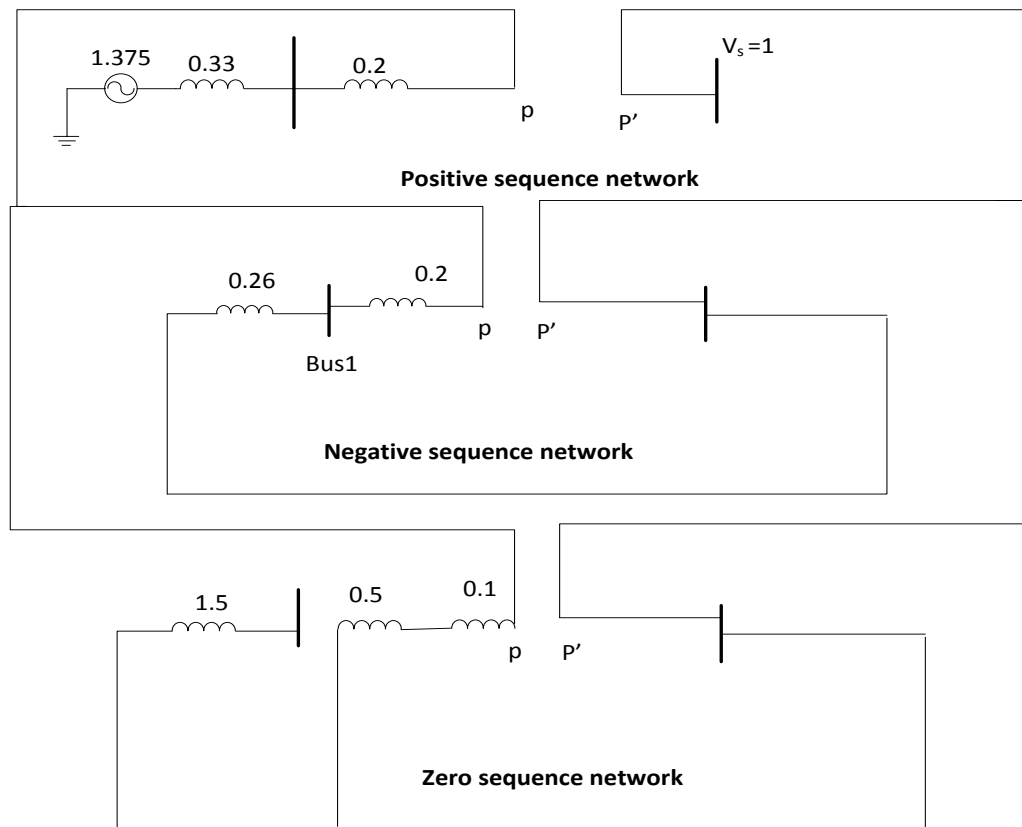
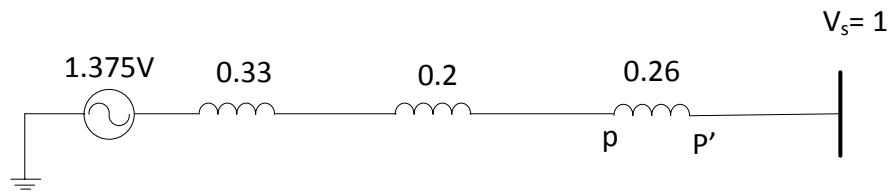


Figure 36: Connection of sequence networks for an open conductor fault

And the network simplifies to:



**Figure 37: Equivalent circuit to be used for analysis of an open conductor fault**

From the figures in the simplified circuit, the power angle characteristic becomes:

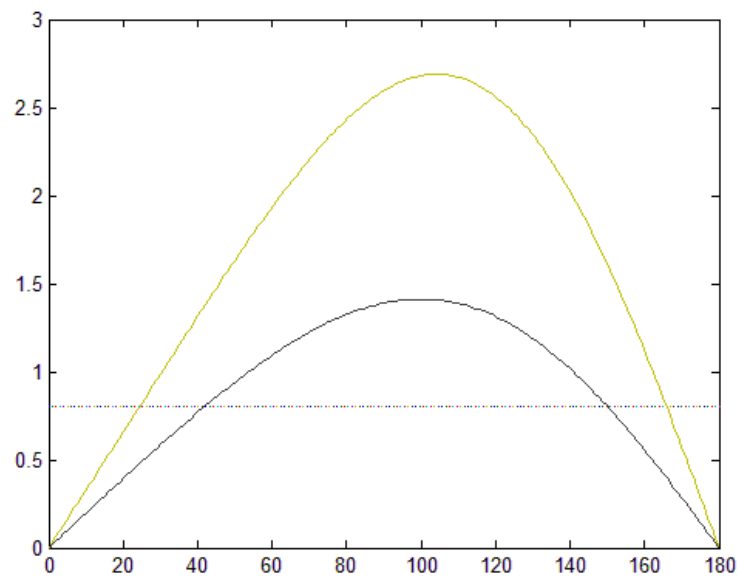


**Figure 38: Power angle characteristic curves for a system before and after the occurrence of the fault**

From the above characteristic, it is clear to see that the stability of the system improves from changing the winding configuration only.

### 7.2.2 SIMPOW Simulation

In the dynamic file DYNPOW, the winding configuration was changed to Delta-Delta as follows:

CP1= D

CP2= Y

The rest of the file parameters are as shown in Appendix G.

The results obtained are as follows:

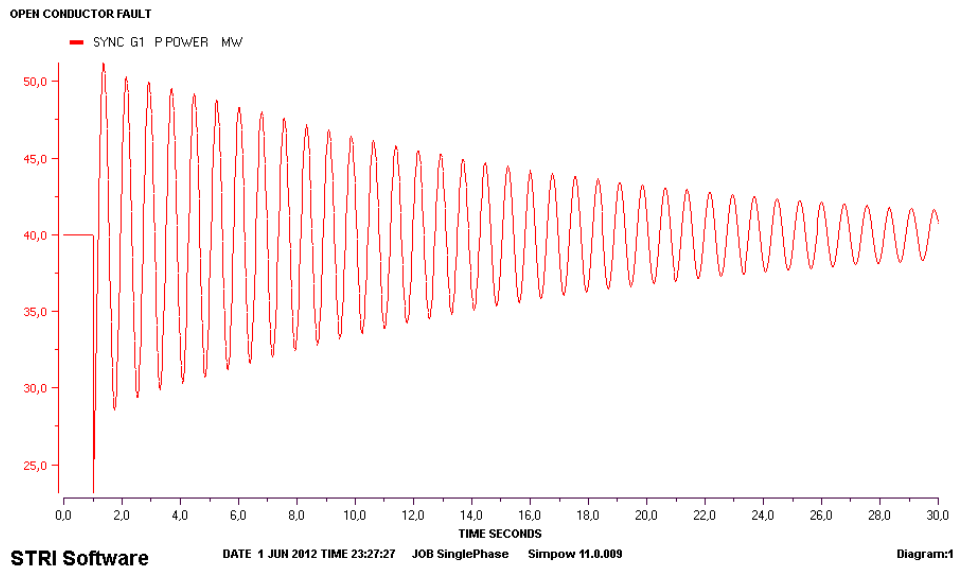


**Figure 39: Power oscillations of the generator after occurrence of a fault**

## 7.3 Discussion

### Grounding

From the circuit parameters given in chapter 6, the adjustments were made in section 7.1 and the zero sequence circuit reactance reduced from 2.5 to 0.3. This resulted in a reduction of the effective reactance which was introduced in the positive sequence network from 0.95 to 0.17. Using this effective reactance, the figure 34 was drawn using Matlab and from SIMPOW simulation, the figure 35 was obtained. The oscillations in figure 29 spiral out of control while in figure 35, the system is stable.

### Transformer Winding Configuration

The graph of figure 39, compared to figure 35, has larger oscillations and the oscillations occur for a longer period. This difference is brought about by the change in winding configuration from Wye-Wye to Delta-Wye configuration. This can be understood from the analytic analysis of the zero sequence network whose reactance increases from 0.3 to 0.6 and therefore increases the effective impedance introduced in the positive sequence network.

## 8. Two Open Conductors Fault: Case Studies

For the sake of completeness, it was decided that the fault involving an open conductor in two of the three phases be investigated. The network that was used for the investigation of two open conductor fault is as shown below.

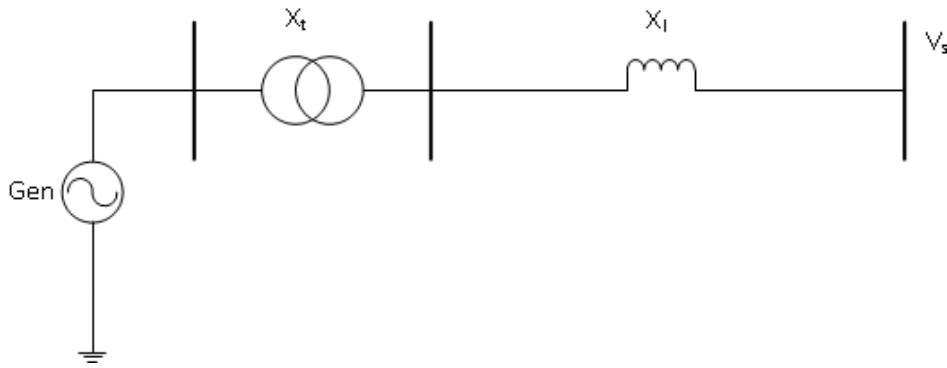


Figure 40: Power system network

A summary of the system parameters is as follows:

### Generator:

$X'_d = 0.25$        $X_2 = 0.26$        $X_0 = 1.5$       Earthed through 0.1 reactance

### Transformer

$X_t = 0.1$        $X_2 = 0.1$        $X_0 = 0.5$       Earthed through 0.5 reactance

### Transmission Line

$X_L = 0.1$        $X_2 = 0.1$        $X_0 = 0.5$

Detailed generator parameters are as shown in appendix A.

The fault was assumed to occur in phases B and C. Just like for the single open conductor fault, the methodology was to undertake an analytic approach and then confirm the results using simulation.

## 8.1 Analytically

Using symmetrical components, the network is resolved into positive, negative and zero sequence circuits as shown below. These sequence networks are connected to each other in series at the point of the fault PP'.

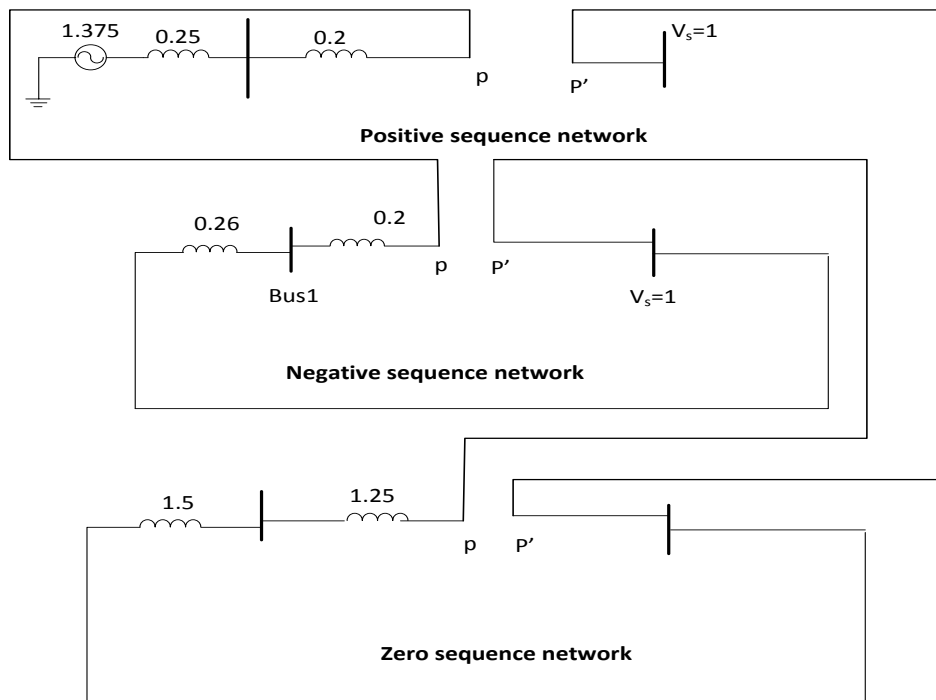


**Figure 41: Connection of sequence networks for two open conductor fault**

The network reduces to

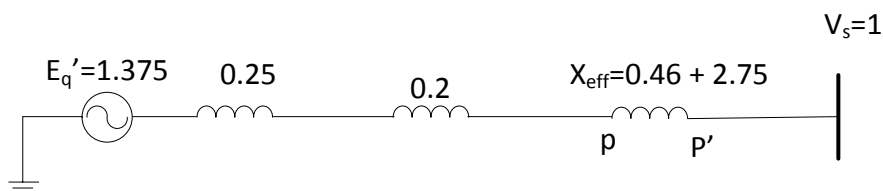


**Figure 42: Connection of sequence networks for two open conductor fault**

Where  $X_{eff}$  is the series connection of the negative and zero sequence circuit reactances.



### 8.1.1 Effect of grounding

If the grounding is improved as follows:

Generator: Reducing  $X_0$  from 1.5 to 0.1 and solidly earthing the neutral.

Transformer: Reducing  $X_{120}$  from 0.5 to 0.1

Both neutrals solidly earthed

Transmission line:  $X_0 = 0.1$

The network reduces to

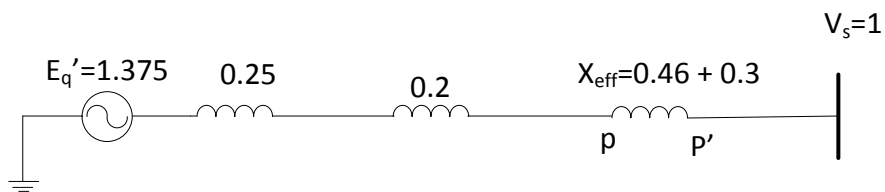
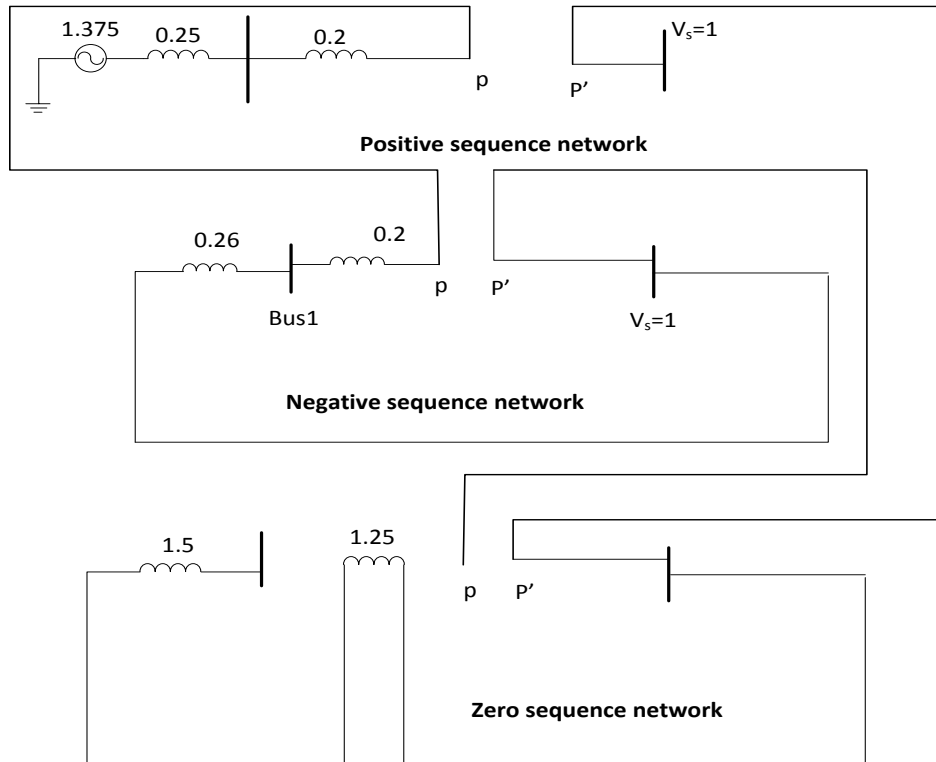


Figure 43: Connection of sequence networks for two open conductor fault

### 8.1.2 Effect of Transformer winding configuration

If the transformer in network of figure 40 and 41 is changed from Wye-Wye to Delta-Wye- ungrounded, then symmetrical components networks are connected as follows.



**Figure 44: Connection of sequence networks for two open conductor fault with a different transformer winding configuration**

The circuit becomes an open circuit.

## 8.2 Simulation using SIMPOW

The power flow program was maintained but the dynamic file was changed to simulate open conductors in phase B and C. The DYNPOW file is attached in appendix H. The power produced from the synchronous machine is reduced from the single conductor case of 0.8pu to 0.2pu. The two open conductor fault is simulated at 1 second after the start of the simulations. The results for the current flows in phases A, B and C for line between bus 3 and bus 4 is shown below.

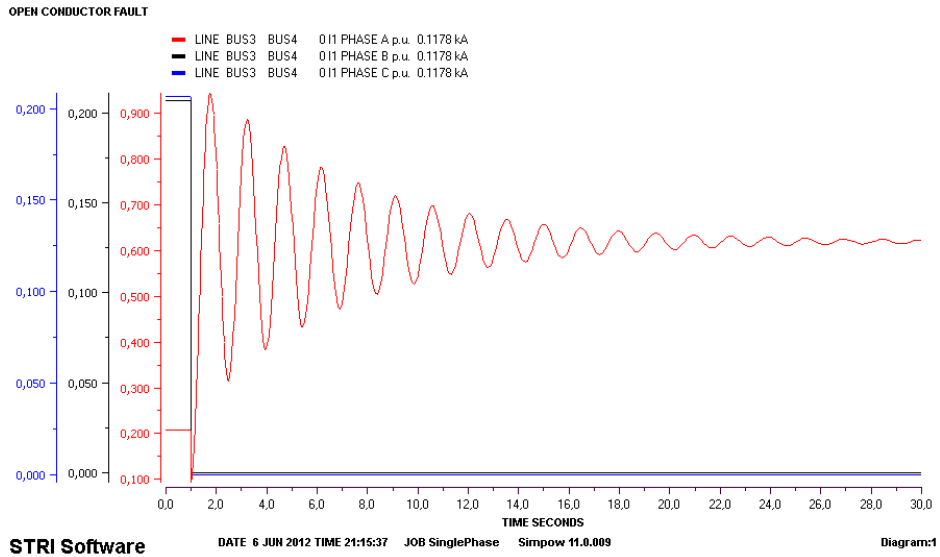


Figure 45: Line currents in phases A, B and C after occurrence of a two open conductor fault

The power flow from the generator is shown below.

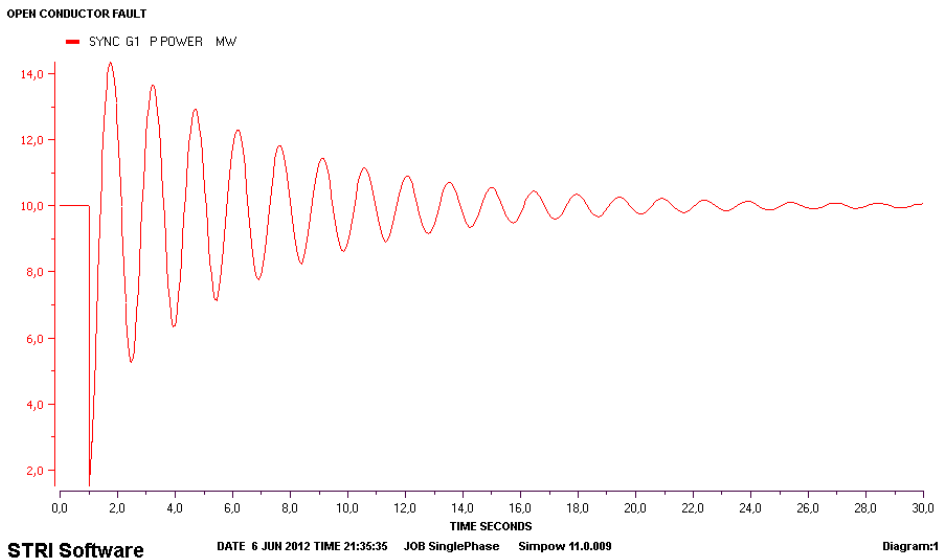


Figure 46: Power oscillations of the generator after occurrence two open conductor fault

### 8.2.1 Effect of grounding

The synchronous machine grounding was changed to un-grounded by removing the neutral earthing in the DYNPOW file. Alternatively, the resistance R0 was set to a very high impedance of 100,000. The result for the power transfer from the synchronous machine to the grid is as shown below.

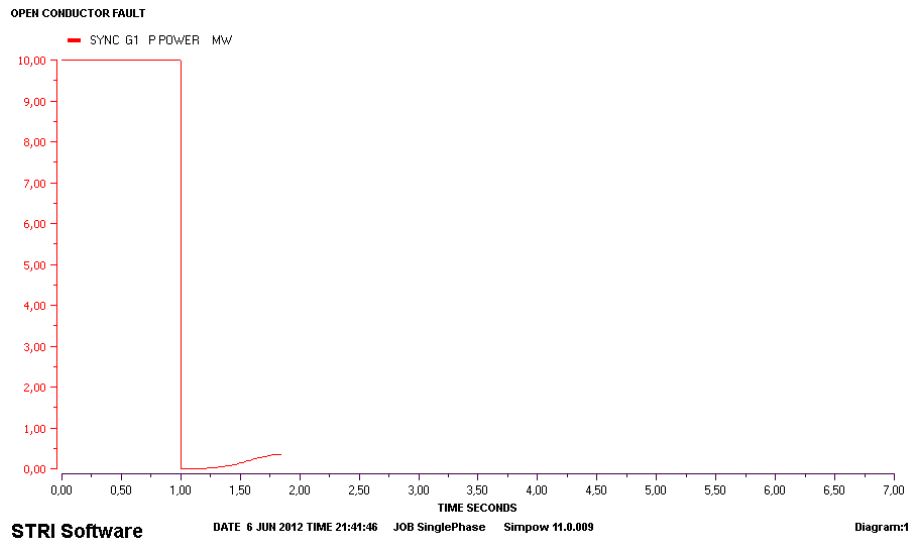


Figure 47: Power flow of the generator after occurrence two open conductor fault

### 8.2.2 Effect of transformer winding configuration

The transformer winding was changed from Wye-Wye to Delta-Delta by changing the **CP1=Y CP2=Y** to **CP1=D CP2=D** in the DYNPOW file. The result which was obtained for the power transfer between the synchronous machine and the infinite grid is as shown below.

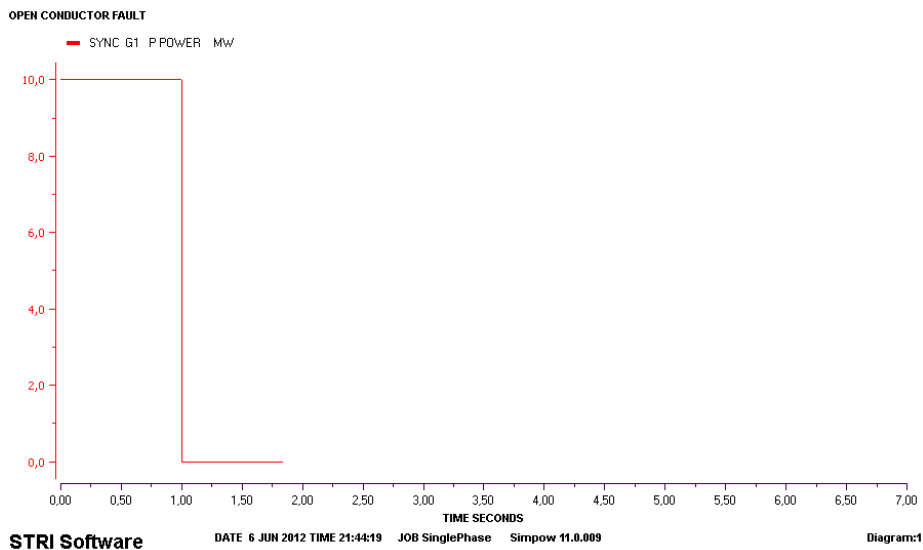


Figure 48: Power flow of the generator after occurrence two open conductor fault

### 8.3 Discussion

It has been demonstrated in this section that the power transfer in a two open conductor fault can only be possible when there is a return path to the generation point. This was shown both analytically and using the power transfer curves from SIMPOW.

From the analytical circuits, it can be seen that the circuit becomes an open circuit during this fault because of the zero sequence circuit which becomes open.

In the SIMPOW simulation, it can be seen in curves shown in figure 47 and 48 that the power transfer ceases within a second of the occurrence of the fault.

## 9. Discussion

In chapter 3, the equations for positive and negative damping power of a power system were discussed and their applicability to open conductor faults established. This theory was applied to specific cases in chapter 5. The results obtained in chapter 5 using the three methods were close especially for cases with reactance in the external circuit. The damping ratio for the Type 2A machine, however, was much poorer than the Type 4 and analytic case. The main finding was that a system with an open conductor fault has poorer damping power compared to a normal operation.

As outlined in chapter 4, an attempt was made to use SIMPOW to draw the power angle curve. This proved to be futile and the analytic method was found to be a suitable method of drawing the power-angle characteristic curve.

Transient stability case study was conducted as discussed in chapter 6. Using Equal Area criterion, an assessment was made of figure 27 and figure 28 in determining the stability of each case. By comparing the accelerating and decelerating areas of each curve, it was possible to determine that the first case was stable while the second was not stable. The main observation in this study is that the open conductor fault increases the accelerating area while reducing the deceleration area of a power system characteristic curve. This can lead to instability when the stability limit of equal areas is reached.

In SIMPOW, the first case was simulated and the result is a curve shown in figure 29. The second case result was obtained as shown in figure 30. It shows a curve of power transfer with uncontrollable oscillations after the occurrence of the fault.

In chapter 7, the issue of grounding and transformer winding configuration change was discussed. The reduced effective reactance which was introduced in the positive sequence network resulted in a system where by the oscillations subsided upon the occurrence of a fault. Similarly, the change in winding configuration was shown to have an impact on the system. In this case, the change in winding configuration from Wye-Wye to Delta-Wye configuration affected the zero sequence network. The reactance increases from 0.3 to 0.6 and therefore increased the effective impedance introduced in the positive sequence network.

Finally in chapter 8, the phenomenon of two open conductor faults was analyzed. From the analytical circuits, it can be seen that the circuit becomes an open circuit during this fault because of the zero sequence circuit which becomes open as a result of poor earthing and the winding configuration of the transformer.

In the SIMPOW simulation, it can be seen in curves shown in figure 47 and 48 that the power transfer ceases within a second of the occurrence of the fault.

## 10. Conclusions

The effect of open conductor faults was studied in detail using symmetrical components. The main conclusions from this study can be summarized as follows:

- The fault can lead to instability of a synchronous machine as was the case in the real event in 2008.
- The line reactance plays a big role in the stability of the system. A weak line connection (or high line reactance) is more likely to result in instability than a stronger one.
- The winding configuration of the transformer plays a vital role in the stability of a system during an open conductor case.
- Grounding of generators, transformers and transmission lines play an important role in stability during this fault.
- A two open conductor case is more severe compared to a single series conductor fault.
- In the case of an unsymmetrical fault, the negative damping torque is more useful to the generator stability than to a motor because it is a retarding torque.
- The negative damping torque is due to the mmf rotating in the clockwise direction (opposite to the direction of machine rotation) at twice the frequency/speed and may lead to increased vibrations of a generator or motor during the fault.

## **11. Recommendations and Further work**

The following work on open conductor faults has been proposed for further work.

1. The study of d-q transformation and the application of it to open conductor fault.
2. The study of effect of open conductor faults on the induction machine
3. The study of multiple faults and the use of the reference frame coordinates
4. A study in to the correctness of the two equations for negative damping torque



## 12. References

- [1] Simon Jorums Mabeta, *Dynamic Analysis of a Synchronous Generator due to an Open Conductor Fault*, TET5500 project course 2011, NTNU
- [2] Kenneth Sjiholt, *Rotor Angle Stability problems for Synchronous Generators connected to a Regional Grid during Open Conductor Fault*, 15th June 2010 Master Thesis 2010, NTNU
- [3] SIMPOW<sup>R</sup> Power Simulation Software User Manual 11.0, also on website [www.simpow.com](http://www.simpow.com) Release date 24<sup>th</sup> September 2010.
- [4] John J. Grainger and William D. Stevenson, Jr., *Power System Analysis*, ISBN 0-07-113338-0, McGraw-Hill
- [5] Jan Machowski, Janusz W. Bialek and James R. Bumby, *Power System Dynamics-Stability and Control*, 2<sup>nd</sup> Ed, John Wiley 2008
- [6] Dr. P. N. Reddy, *Symmetrical components and short circuit studies*, 2<sup>nd</sup> Edition, Khanna Publishers, 1985
- [7] J.C. Das, *Power System Analysis: Short Circuit Load Flow and Harmonics*, 2002 copyright by Marcel Dekker, Inc
- [8] E. W. Kimbark, *Power System Stability Volume 1: Elements of stability calculations*, 1995 reprint by IEEE Press, 1948 copyright.
- [9] E. W. Kimbark, *Power System Stability Volume 3: Synchronous Machines*, 1995 reprint by IEEE Press, 1948 copyright.
- [10] R. H. Park, *Two Reaction Theory of Synchronous Machines – Generalized method of Analysis – Part 1*, A.I.E.E. 1929 Winter convention, New York
- [11] R. H. Park, *Two Reaction Theory of Synchronous Machines – Part 1*, A.I.E.E. 1933 Winter convention, New York
- [12] R. E. Doherty and C. A. Nickle, *Synchronous Machines – 3*, A.I.E.E., 7-11 February 1927, Winter convention, New York
- [13] O. G. C. Dahl, *Electric Power Circuits, Theory and Applications, Volume 2 – Power System Stability*, 1<sup>st</sup> Edition 1938, McGraw-Hill Book company.
- [14] M. M. Liwshitz, *Positive and Negative Damping in Synchronous Machines*, A.I.E.E., 27-31 January 1941 Winter Convention, Philadelphia

- [15] S.B. Crary, *Power System Stability Volume 2 – Transient Stability*, 1947 edition, John Wiley & Sons.
- [16] A.E. Fitzgerald, C. Kingsley, S.D. Umans, *Electric Machinery*, 1983 edition, McGraw-Hill
- [17] John Hindmarsh, Alasdair Renfrew, *Electric Machines and Drive Systems*, 1996 3rd Edition, Butterworth-Heinemann
- [18] Prabha Kundur, *Power System Stability and control*, EPR Institute, 1979, McGraw-Hill
- [19] Chee-Mun Ong, *Dynaminc Simulation of Electric Machinery using Matlab/Simulink*, 1998 Prentice Hall, ISBN 0-13-723785-5
- [20] P. L. Alger, *Induction Machines*, 2<sup>nd</sup> Edition G&B publishers, 1970 New York.
- [21] R. E. Doherty and C. A. Nickle, *Synchronous Machines – 3*, A.I.E.E., 7-11 February 1927, Winter convention, New York
- [22] Kjetil Uhlen, *Power System Stability TET4180 Lecture notes*, NTNU 2011
- [23] Arne T. Holen, Olav B. Fooso and Kjetil Uhlen, *Power System Analysis TET4115 Lecture Notes*, NTNU 2010
- [24] Steinar Danielsen, *Electric Traction Power System Stability*, Doctoral Thesis NTNU 2010

## **13. Appendices**

Appendix A: Synchronous Machine Parameters

Appendix B: OPTPOW & DYNPOW files for the power angle characteristic curve

Appendix C: DYNPOW Power angle curves for round rotor synchronous machine

Appendix D: SIMPOW files for damping coefficient simulation

Appendix E: SIMPOW files for Transient stability simulation

Appendix F: DYNPOW file for power system grounding simulation

Appendix G: DYNPOW file winding configuration simulation

Appendix H: DYNPOW file for two open-conductor fault simulation

Appendix I: Power Angle Characteristic curves using SIMPOW for case study in chapter 4

Appendix J: Matlab File (m file and data file) used for calculations

## 13.1 Appendix A: Synchronous Machine Parameters

### A.1 Salient Pole Generator

Power rating,  $S = 50$  MVA,

Generator Voltage,  $U = 10$  kV

Machine Reactances

$X_d = 1.05$  pu,       $X_d' = 0.328$        $X_d'' = 0.254$ ,

$X_q = 0.66$  pu       $X_q'' = 0.273$

Time constants

$T_{do}' = 2.49$        $T_{do}'' = 0.06$        $T_{qo}'' = 0.15$

Inertia constant,  $H = 3.1$

### A.2 Round Rotor Generator

Power rating,  $S = 50$  MVA,

Generator Voltage,  $U = 10$  kV

Machine Reactances

$X_d = 1.65$  pu,       $X_d' = 0.23$ ,       $X_d'' = 0.17$ ,

$X_q = 1.65$  pu       $X_q' = 0.38$        $X_q'' = 0.17$

Time constants

$T_{do}' = 4.7$        $T_{do}'' = 0.027$        $T_{qo}'' = 0.056$

Inertia Constant,  $H = 3.1$

## 13.2 Appendix B: SIMPOW Files for Power Angle Characteristic curve

### OPTPOW File

\*\*

#### GENERAL

SN=50

END

#### NODES

BUS1 UB=10

BUS2 UB=10

END

#### LINES

BUS1 BUS2 TYPE=0

END

#### POWER CONTROL

BUS1 TYPE=NODE RTYPE=PQ P=40 Q=30 NAME=Gen

BUS2 TYPE=NODE RTYPE=SW U=10 FI=0 NAME=Stiff

END

END

## DYNPOW file

\*\*

### CONTROL DATA

TEND=100

END

### GENERAL

FN=50

REF=STIFF

END

### NODES

BUS2 NAME=STIFF TYPE=1

END

### SYNCHRONOUS MACHINE

G1 BUS1 TYPE=2A XD=1.05 XQ=0.66 XA=0.1 XDP=0.33

XDB=0.25 XQB=0.25 TDOP=2.49 X2=0.26 TDOB=0.06 TQOB=0.15

TURB=2 R0=0 H=3.1 SN=50 UN=10 VREG=0

END

### REGULATORS

1 TYPE=DSL/EXCITERAC8B/ E1=2.222 SE1=1.346 E2=2.962 SE2=1.9

TE=0.8 KE=1.0 TA=0 VRMIN=0 VRMAX=10 KA=1.0 !KA=3.0

TD=0.01 KD=46 KI=140.85 KP=154.2

END

### DSL-TYPES

!Voltage regulator (AVR)

EXCITERAC8B(E1,SE1,E2,SE2,VC,TI/1/,TE,KE,TA,VRMIN,VRMAX,KA,TD,KD,KI,KP,UF,UFO)

END

## **TURBINES**

1 TYPE = ST1 GOV=10 TC = 0.3 KH = 0.6 TR 7

10 TYPE = SGC YMAX=1 YMIN = -1 K = 20 T1 = 0.1

2 TYPE =22 TAB=1

END

## **TABLES**

1 TYPE=0 F 0 1

100 1

END

## **LINES**

BUS1 BUS2 1BREAKER=1

END

## **BREAKERS**

1 TYPE=0 RA=0 RB=0 RC=0 XA=0 XB=0 XC=0

END

## **RUN INSTRUCTION**

AT 1.000 INST OPEN LINE BUS1 BUS2 1BREAKER PHASE 1

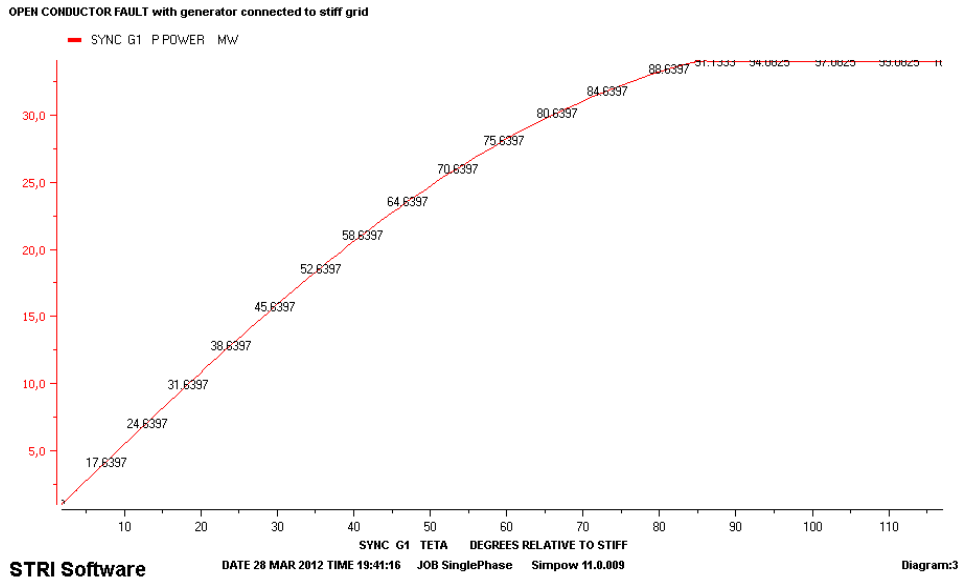
!AT 4.000 INST CLOSE LINE BUS1 BUS2 1BREAKER PHASE 1

END

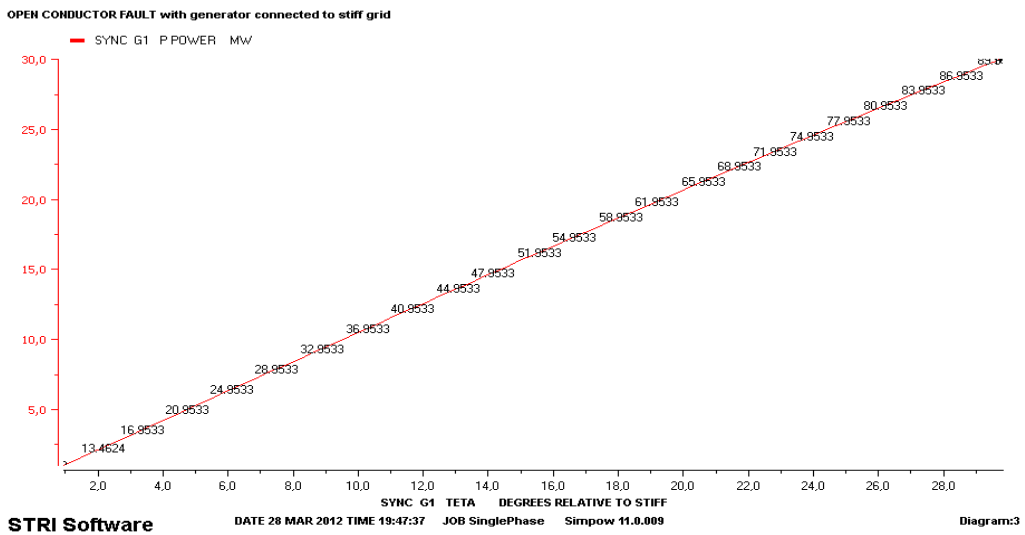
END

### 13.3 Appendix C: Power-Angle Curves for Round Rotor Synchronous Machine

No AVR, Low reactive power Q



No AVR, High reactive power Q





## 13.4 Appendix D: SIMPOW files for damping coefficient simulation

OPTPOW file for both type 4 and 2A synchronous machines

\*\*

### GENERAL

SN=50

END

### NODES

BUS1 UB=10

BUS2 UB=10

BUS3 UB=10

END

### LINES

BUS1 BUS2 TYPE=0

BUS2 BUS3 TYPE=1 X=0.001 L=1

END

### POWER CONTROL

BUS1 TYPE=NODE RTYPE=PQ P=40 Q=30 NAME=Gen

BUS3 TYPE=NODE RTYPE=SW U=10 FI=0 NAME=Stiff

END

END

## DYNPOW file for Type 4 synchronous machine

\*\*

### CONTROL DATA

TEND=10

END

### GENERAL

FN=50

REF=STIFF

END

### NODES

BUS3 NAME=STIFF TYPE=1

END

### SYNCHRONOUS MACHINE

G1 BUS1 TYPE=4 XD=1.05 XQ=0.66 XA=0.0010 XDP=0.33

SN=50 UN=10

D=12.9 H=3.1

END

### LINES

BUS2 BUS3 1BREAKER=1

END

### BREAKERS

1 TYPE=0 RA=0 RB=0 RC=0 XA=0 XB=0 XC=0

END

### RUN INSTRUCTION

AT 1.000 INST OPEN LINE BUS2 BUS3 1BREAKER PHASE 1

!AT 4.000 INST CLOSE LINE BUS2 BUS3 1BREAKER PHASE 1

END

END

DYNPOW file for Type 2A synchronous machine.

\*\*

**CONTROL DATA**

TEND=10

END

**GENERAL**

FN=50

REF=STIFF

END

**NODES**

BUS3 NAME=STIFF TYPE=1

END

**SYNCHRONOUS MACHINE**

G1 BUS1 TYPE=2A XD=1.05 XQ=0.66 XA=0.10 XDP=0.328

XDB=0.254 XQB=0.273 TD0P=2.49

TD0B=0.06 TQ0B=0.15 TURB=2 X0=100

H=3.1 SN=50 UN=10 VREG=0

END

**REGULATORS**

1 TYPE=DSL/EXCITERAC8B/ E1=2.222 SE1=1.346 E2=2.962 SE2=1.9

TE=0.8 KE=1.0 TA=0 VRMIN=0 VRMAX=10 KA=1.0 !KA=3.0

TD=0.01 KD=46 KI=140.85 KP=154.2

END

**DSL-TYPES**

!Voltage regulator (AVR)

EXCITERAC8B(E1,SE1,E2,SE2,VC,TI/1/,TE,KE,TA,VRMIN,VRMAX,KA,TD,KD,KI,KP,UF,UFO)

END

## **TURBINES**

1 TYPE = ST1 GOV=10 TC = 0.3 KH = 0.6 TR 7

10 TYPE = SGC YMAX=1 YMIN = -1 K = 20 T1 = 0.1

2 TYPE = 22 TAB=1

END

## **TABLES**

1 TYPE=0 F 0 1

100 1

END

## **LINES**

BUS1 BUS2 1BREAKER=1

END

## **BREAKERS**

1 TYPE=0 RA=0 RB=0 RC=0 XA=0 XB=0 XC=0

END

## **RUN INSTRUCTION**

!AT 1.000 INST OPEN LINE BUS1 BUS2 1BREAKER PHASE 1

!AT 6.000 INST CLOSE LINE BUS1 BUS2 1BREAKER PHASE 1

END

END

## 13.5 Appendix E: SIMPOW files for Transient stability simulation

### OPTPOW File

\*\*

#### GENERAL

SN=50

END

#### NODES

BUS1 UB=10

BUS2 UB=10

BUS3 UB=245

BUS4 UB=245

END

#### LINES

BUS1 BUS2 TYPE=0

BUS3 BUS4 TYPE=1 X=0.4 L=300

END

#### TRANSFORMERS

BUS2 BUS3 SN=50 UN1=10 UN2=245 EX12=0.1 ER12=0

END

#### POWER CONTROL

BUS1 TYPE=NODE RTYPE=PQ P=40 Q=30 NAME=Gen

BUS4 TYPE=NODE RTYPE=SW U=245 FI=0 NAME=Stiff

END

END

## DYNPOW File

\*\*

### CONTROL DATA

TEND=30

END

### GENERAL

FN=50

REF=STIFF

END

### NODES

BUS4 NAME=STIFF TYPE=1

END

### TRANSFORMERS

BUS2 BUS3 CP1=Y CP2=Y

EX120=0.5

RN1=0.01 RN2=0.0003

END

### LINES

BUS3 BUS4 X0 0.5

END

### SYNCHRONOUS MACHINE

G1 BUS1 TYPE=2A XD=1.05 XQ=0.66 XA=0.10 XDP=0.328

XDB=0.254 XQB=0.273 TDOP=2.49 TD0B=0.06

TQ0B=0.15 X2=0.27 X0=1.5 TURB=1

H=3.1 SN=50 UN=10 VREG=1

END

## REGULATORS

1 TYPE=DSL/EXCITERAC8B/ E1=2.222 SE1=1.346 E2=2.962 SE2=1.9

TE=0.8 KE=1.0 TA=0 VRMIN=0 VRMAX=10 KA=1.0 !KA=3.0

TD=0.01 KD=46 KI=140.85 KP=154.2

END

## DSL-TYPES

!Voltage regulator (AVR)

EXCITERAC8B(E1,SE1,E2,SE2,VC,TI/1/,TE,KE,TA,VRMIN,VRMAX,KA,TD,KD,KI,KP,UF,UFO)

END

## TURBINES

1 TYPE = ST1 GOV=10 TC = 0.3 KH = 0.6 TR 7

10 TYPE = SGC YMAX=1 YMIN = -1 K = 20 T1 = 0.1

END

## LINES

BUS3 BUS4 1BREAKER=1

END

## BREAKERS

1 TYPE=0 RA=0 RB=0 RC=0 XA=0 XB=0 XC=0

END

## RUN INSTRUCTION

AT 1.000 INST OPEN LINE BUS3 BUS4 1BREAKER PHASE 1

!AT 6.000 INST CLOSE LINE BUS3 BUS4 2BREAKER PHASE 1

END

END

## 13.6 Appendix F: DYNPOW file for power system grounding simulation

\*\*

### CONTROL DATA

TEND=100

END

### GENERAL

FN=50

REF=STIFF

END

### NODES

BUS4 NAME=STIFF TYPE=1

END

### TRANSFORMERS

BUS2 BUS3 CP1=Y CP2=Y

EX120=0.1

RN1=0 RN2=0

END

### LINES

BUS3 BUS4 X0 0.5

END

### SYNCHRONOUS MACHINE

G1 BUS1 TYPE=2A XD=1.05 XQ=0.66 XA=0.10 XDP=0.328

XDB=0.254 XQB=0.273 TD0P=2.49 TD0B=0.06

TQ0B=0.15 X2=0.26 X0=0.1 TURB=1

H=3.1 SN=50 UN=10 VREG=1

END



## REGULATORS

1 TYPE=DSL/EXCITERAC8B/ E1=2.222 SE1=1.346 E2=2.962 SE2=1.9

TE=0.8 KE=1.0 TA=0 VRMIN=0 VRMAX=10 KA=1.0

TD=0.01 KD=46 KI=140.85 KP=154.2

END

## DSL-TYPES

!Voltage regulator (AVR)

EXCITERAC8B(E1,SE1,E2,SE2,VC,TI/1/,TE,KE,TA,VRMIN,VRMAX,KA,TD,KD,KI,KP,UF,UFO)

END

## TURBINES

1 TYPE = ST1 GOV=10 TC = 0.3 KH = 0.6 TR 7

10 TYPE = SGC YMAX=1 YMIN = -1 K = 20 T1 = 0.1

2 TYPE =22 TAB=1

END

## LINES

BUS3 BUS4 1BREAKER=1

END

## BREAKERS

1 TYPE=0 RA=0 RB=0 RC=0 XA=0 XB=0 XC=0

END

## RUN INSTRUCTION

!Simulating the open conductor fault after 1 second

AT 1.000 INST OPEN LINE BUS3 BUS4 1BREAKER PHASE 1

!AT 6.000 INST CLOSE LINE BUS3 BUS4 2BREAKER PHASE 1

END

END

## 13.7 Appendix G: DYNPOW file winding configuration simulation

\*\*

### CONTROL DATA

TEND=30

END

### GENERAL

FN=50

REF=STIFF

END

### NODES

BUS4 NAME=STIFF TYPE=1

END

### TRANSFORMERS

BUS2 BUS3 CP1=D CP2=Y

EX120=0.5

RN1=0.01 RN2=0.0003

END

### LINES

BUS3 BUS4 X0 3.5

END

### SYNCHRONOUS MACHINE

G1 BUS1 TYPE=2A XD=1.05 XQ=0.66 XA=0.10 XDP=0.328

XDB=0.254 XQB=0.273 TDOP=2.49 TDOB=0.06

TQOB=0.15 X2=0.26 X0=1.5 TURB=1

H=3.1 SN=50 UN=10 VREG=1

END

## REGULATORS

1 TYPE=DSL/EXCITERAC8B/ E1=2.222 SE1=1.346 E2=2.962 SE2=1.9

TE=0.8 KE=1.0 TA=0 VRMIN=0 VRMAX=10 KA=1.0 !KA=3.0

TD=0.01 KD=46 KI=140.85 KP=154.2

END

## DSL-TYPES

!Voltage regulator (AVR)

EXCITERAC8B(E1,SE1,E2,SE2,VC,TI/1/,TE,KE,TA,VRMIN,VRMAX,KA,TD,KD,KI,KP,UF,UFO)

END

## TURBINES

1 TYPE = ST1 GOV=10 TC = 0.3 KH = 0.6 TR 7

10 TYPE = SGC YMAX=1 YMIN = -1 K = 20 T1 = 0.1

2 TYPE =22 TAB=1

END

## LINES

BUS3 BUS4 1BREAKER=1

END

## BREAKERS

1 TYPE=0 RA=0 RB=0 RC=0 XA=0 XB=0 XC=0

END

## RUN INSTRUCTION

AT 1.000 INST OPEN LINE BUS3 BUS4 1BREAKER PHASE 1

!AT 6.000 INST CLOSE LINE BUS3 BUS4 2BREAKER PHASE 1

END

END

## 13.8 Appendix H: DYNPOW file for two open-conductor fault simulation

\*\*

### CONTROL DATA

TEND=30

END

### GENERAL

FN=50

REF=STIFF

END

### NODES

BUS4 NAME=STIFF TYPE=1

END

### TRANSFORMERS

BUS2 BUS3 CP1=Y CP2=Y

EX120=0.5

RN1=0.01 RN2=0.0003

END

### LINES

BUS3 BUS4 X0 0.5

END

### SYNCHRONOUS MACHINE

G1 BUS1 TYPE=2A XD=1.05 XQ=0.66 XA=0.10 XDP=0.328

XDB=0.254 XQB=0.273 TDOP=2.49 TD0B=0.06

TQ0B=0.15 X2=0.26 X0=1.5 R0=0 TURB=1

H=3.1 SN=50 UN=10 VREG=1

END

## REGULATORS

1 TYPE=DSL/EXCITERAC8B/ E1=2.222 SE1=1.346 E2=2.962 SE2=1.9

TE=0.8 KE=1.0 TA=0 VRMIN=0 VRMAX=10 KA=1.0 !KA=3.0

TD=0.01 KD=46 KI=140.85 KP=154.2

END

## DSL-TYPES

EXCITERAC8B(E1,SE1,E2,SE2,VC,TI/1/,TE,KE,TA,VRMIN,VRMAX,KA,TD,KD,KI,KP,UF,UFO)

END

## TURBINES

1 TYPE = ST1 GOV=10 TC = 0.3 KH = 0.6 TR 7

10 TYPE = SGC YMAX=1 YMIN = -1 K = 20 T1 = 0.1

END

## LINES

BUS3 BUS4 1BREAKER=1

END

## BREAKERS

1 TYPE=0 RA=0 RB=0 RC=0 XA=0 XB=0 XC=0

END

## RUN INSTRUCTION

AT 1.000 INST OPEN LINE BUS3 BUS4 1BREAKER PHASE 23

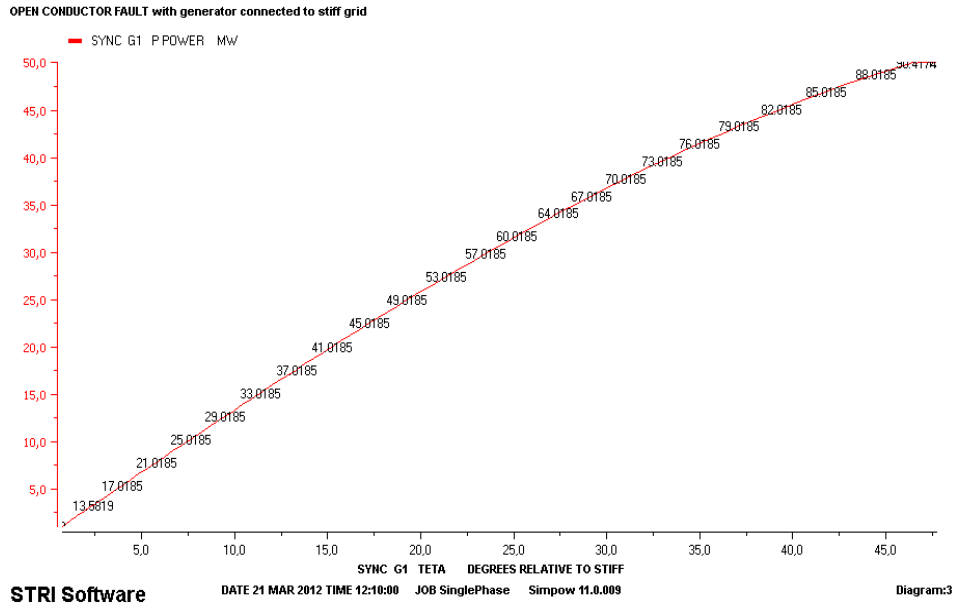
!AT 2.500 INST CLOSE LINE BUS3 BUS4 1BREAKER PHASE 23

END

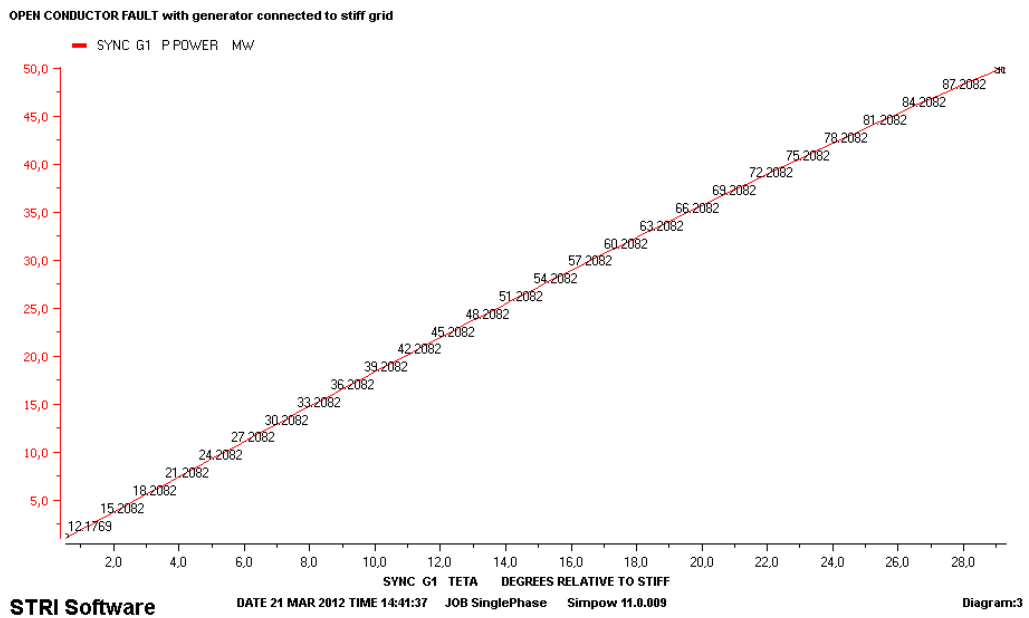
END

# 13.9 Appendix I: Power Angle Characteristic curves using SIMPOW for case study in chapter 4

No AVR, Low Q

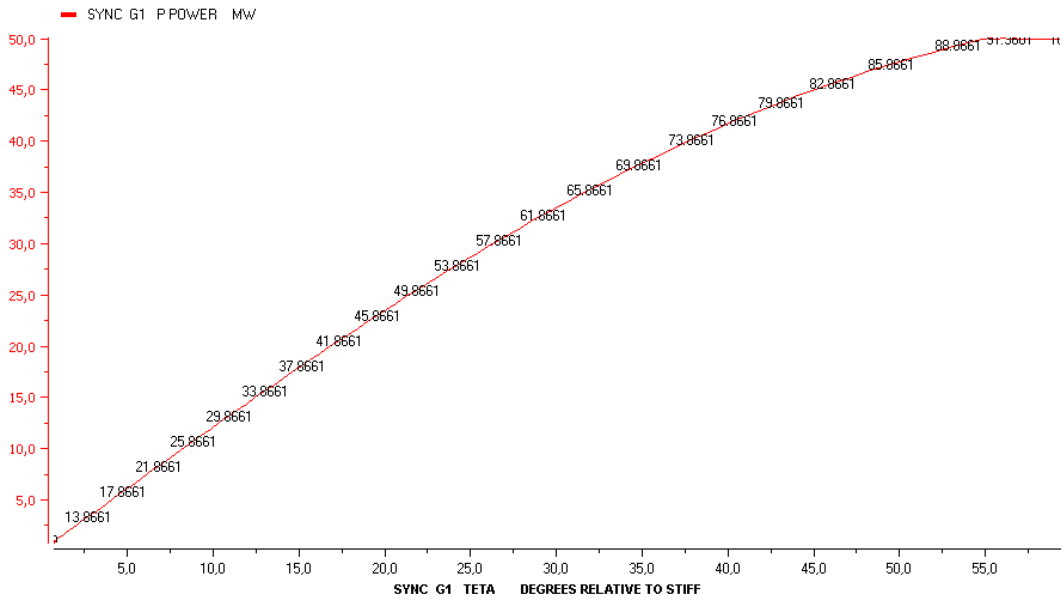


No AVR, High Q



No AVR, Low Q with an open conductor fault.

**OPEN CONDUCTOR FAULT with generator connected to stiff grid**



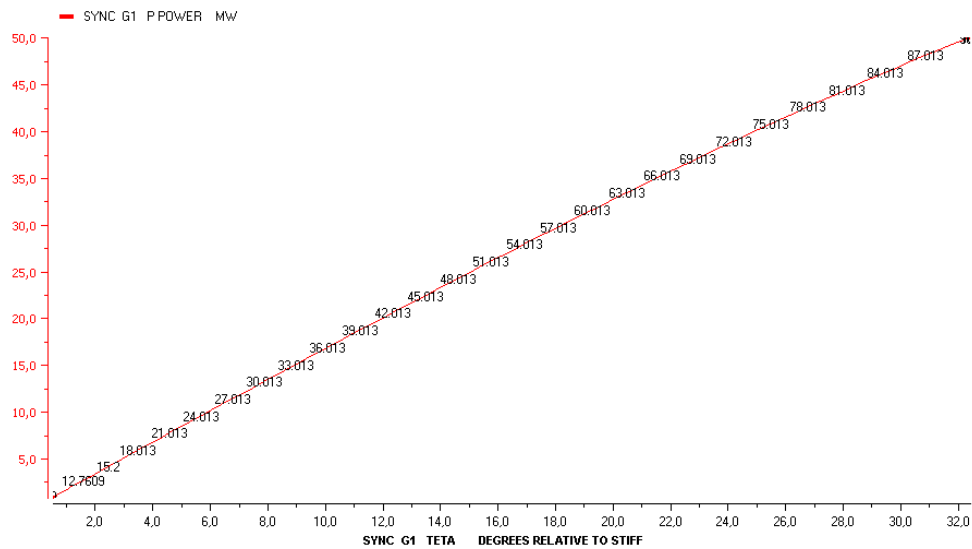
STR1 Software

DATE 21 MAR 2012 TIME 15:45:07 JOB SinglePhase Simpov 11.0.009

Diagram:3

No AVR, High Q, with open conductor.

**OPEN CONDUCTOR FAULT with generator connected to stiff grid**



STR1 Software

DATE 21 MAR 2012 TIME 15:52:08 JOB SinglePhase Simpov 11.0.009

Diagram:3

## Appendix J: Matlab File used for calculations.

```

% Grid connected synchronous generator
% No transmission line, Steady state
% To run the script you must define I, reactances and time constants
Vs=1+0j
xq=Xq+X
xd=Xd+X
xqp=Xqp+X
xdp=Xdp+X
EQ=Vs+j*xq*I
delta=atan(imag(EQ)/real(EQ));
deltadeg=delta*180/pi
fi=atan(-imag(I)/real(I));
fideg=-fi*180/pi
Id=-abs(I)*sin(delta+fi)
Eq=Vs*cos(delta)+(-xd*Id)
Eqp=Vs*cos(delta)+(-xdp*Id)
Peq=Vs*Eq/xd*sin(delta)+0.5*Vs^2*(1/xq-1/xd)*sin(2*delta)
Peqp=Vs*Eqp/xdp*sin(delta)+0.5*Vs^2*(1/xqp-1/xdp)*sin(2*delta)
OCFPeqp=Vs*Eqp/(xdp+Xeff)*sin(delta)+0.5*Vs^2*(1/(xqp+Xeff)-
1/(xdp+Xeff))*sin(2*delta)
KEq=Vs*Eq/xd*cos(delta)+Vs^2*(1/xq-1/xd)*cos(2*delta)
KEqp=Vs*Eqp/xdp*cos(delta)+Vs^2*(1/xqp-1/xdp)*cos(2*delta)
OCFKEqp=Vs*Eqp/(xdp+Xeff)*cos(delta)+Vs^2*(1/(xqp+Xeff)-
1/(xdp+Xeff))*cos(2*delta)
Dd=Vs^2*((Xdp-Xdb)*Td0b/(X+Xdp)^2);
Dq=Vs^2*((Xqp-Xqb)*Tq0b/(X+Xqp)^2);
OCFDd=Vs^2*((Xdp-Xdb)*Td0b/(X+Xeff+Xdp)^2);
OCFDq=Vs^2*((Xqp-Xqb)*Tq0b/(X+Xeff+Xqp)^2);
D=(Dd*(sin(delta))^2+Dq*(cos(delta))^2)*100*pi
OCFD=(OCFDd*(sin(delta))^2+OCFDq*(cos(delta))^2)*100*pi
DRatio=D/(2*sqrt(2*H*KEqp*314))*100
OCFDRatio=OCFD/(2*sqrt(2*H*OCFKEqp*314))*100
Dn=(In^2*(r2-r1))*100*pi
Lambda=-D/(4*H)+j*sqrt(KEqp*100*pi/(2*H)-((D/(4*H))^2))
LambdaS=-D/(4*H)+sqrt((D/(4*H))^2)-(KEqp*100*pi/(2*H)))/(2*pi)
OCFLambda=-OCFD/(4*H)+j*sqrt(OCFKEqp*100*pi/(2*H)-((OCFD/(4*H))^2))
OCFLambdaS=-OCFD/(4*H)+j*sqrt(OCFKEqp*100*pi/(2*H)-((OCFD/(4*H))^2))/(2*pi)
dvector=linspace(0,pi,180);
figure(1);
plot(dvector*180/pi,Vs*Eq/xd*sin(dvector)+0.5*Vs^2*(1/xq-
1/xd)*sin(2*dvector),dvector*180/pi,Vs*Eqp/xdp*sin(dvector)+0.5*Vs^2*(1/xqp-
1/xdp)*sin(2*dvector))
figure(2);
plot(dvector*180/pi,0.8,dvector*180/pi,Vs*Eqp/xdp*sin(dvector)+0.5*Vs^2*(1/
xqp-
1/xdp)*sin(2*dvector),dvector*180/pi,Vs*Eqp/(xdp+Xeff)*sin(dvector)+0.5*Vs^
2*(1/(xqp+Xeff)-1/(xdp+Xeff))*sin(2*dvector))

```



Data file used in the Matlab file

<b>Parameter</b>	<b>Variable</b>	
Infinite grid voltage	Vs	1
Load current	I	0.8-j0.6
Quadrature reactance	xq	0.66
Direct reactance	xd	1.05
Transient Quadrature reactance	xqp	0.66
Transient Direct reactance	xdp	0.33
Sub-transient Quadrature reactance	xqb	0.25
Sub-transient Direct reactance	xdb	0.25
Inertia constant	H	3.1
Negative sequence current	In	
External reactance	X	
Positive sequence resistance	r1	0.005
Negative sequence resistance	r2	0.12